Cellular Microbiology (2009) **11**(7), 1044–1063
doi:10.1111/j.1462-5822.2009.01306.x
First published online 27 March 2009

HadA is an atypical new multifunctional trimeric coiled-coil adhesin of *Haemophilus influenzae* biogroup *aegyptius*, which promotes entry into host cells

Davide Serruto,[1‡] Tiziana Spadafina,[1‡] Maria Scarselli,[1] Stefania Bambini,[1] Maurizio Comanducci,[1] Sonja Höhle,[2] Mogens Kilian,[2] Esteban Veiga,[3,4,5†] Pascale Cossart,[3,4,5] Marco R. Oggioni,[6] Silvana Savino,[1] Ilaria Ferlenghi,[1] Anna Rita Taddei,[7] Rino Rappuoli,[1] Mariagrazia Pizza,[1] Vega Masignani[1] and Beatrice Aricò[1*]

[1]*Research Center, Novartis Vaccines and Diagnostics, 53100 Siena, Italy.*
[2]*Department of Medical Microbiology and Immunology, Aarhus University, The Bartholin Building, DK-8000 Aarhus, Denmark.*
[3]*Institut Pasteur, Unité des Interactions Bactéries-Cellules, Paris F-75015, France.*
[4]*INSERM, U604, Paris F-75015, France.*
[5]*INRA, USC2020, Paris F-75015, France.*
[6]*Laboratorio di Microbiologia Molecolare e Biotecnologia, Dipartimento di Biologia Molecolare, University of Siena, 53100 Siena, Italy.*
[7]*Centro Interdipartimentale di Microscopia Elettronica, University of Tuscia, 01100 Viterbo, Italy.*

Summary

The Oca (Oligomeric coiled-coil adhesin) family is a subgroup of the bacterial trimeric autotransporter adhesins, which includes structurally related proteins, such as YadA of *Yersinia enterocolitica* and NadA of *Neisseria meningitidis*. In this study, we searched *in silico* for novel members of this family in bacterial genomes and identified HadA (*Haemophilus* adhesin A), a trimeric autotransporter expressed only by *Haemophilus influenzae* biogroup *aegyptius* causing Brazilian purpuric fever (BPF), a fulminant septicemic disease of children. By comparative genomics and sequence analysis we predicted that the *hadA* gene is harboured on a mobile genetic element unique to BPF isolates. Biological analysis of HadA in the native background was limited because this organism is not amenable to genetic manipulation. Alternatively, we demonstrated that expression of HadA confers to a non-invasive *Escherichia coli* strain the ability to adhere to human cells and to extracellular matrix proteins and to induce *in vitro* bacterial aggregation and microcolony formation. Intriguingly, HadA is predicted to lack the typical N-terminal head domain of Oca proteins generally associated with cellular receptor binding. We propose here a structural model of the HadA coiled-coil stalk and show that the N-terminal region is still responsible of the binding activity and a KGD motif plays a role. Interestingly, HadA promotes bacterial entry into mammalian cells. Our results show a cytoskeleton re-arrangement and an involvement of clathrin in the HadA-mediated internalization. These data give new insights on the structure-function relationship of oligomeric coiled-coil adhesins and suggest a potential role of this protein in the pathogenesis of BPF.

Received 25 September, 2008; revised 19 February, 2009; accepted 20 February, 2009. *For correspondence. E-mail beatrice.arico@novartis.com; Tel. (+39) 0577 243088; Fax (+39) 0577 243564.
†Present address: Dto. Inmunología, primera planta, Hospital de la Princesa, 28006 Madrid, Spain.
‡These authors contributed equally to this work.

Introduction

The recently recognized 'oligomeric coiled-coil adhesin' (Oca) family belongs to the wider family of trimeric autotransporter adhesins (TAAs) characterized by the ability to form highly stable trimers on the bacterial surface and by a common mechanism of secretion, which is linked to their trimerization (Surana *et al.*, 2004; Cotter *et al.*, 2005; Linke *et al.*, 2006). To date, all of them appear to have adhesive activity that is involved in mediating bacterial interaction with either host cells or extracellular matrix (ECM) proteins and in some cases in inducing invasion of target cells (Yang and Isberg, 1993; McMichael *et al.*, 1998; Eitel and Dersch, 2002; Laarmann *et al.*, 2002; Ray *et al.*, 2002; Roggenkamp *et al.*, 2003; Li

et al., 2004; Riess *et al*., 2004; Zhang *et al*., 2004; Capecchi *et al*., 2005; Girard and Mourez, 2006; Heise and Dersch, 2006; Scarselli *et al*., 2006).

Despite the limited degree of sequence similarity, Oca proteins share a similar topology consisting of a conserved C-terminal membrane anchor through which the protein is translocated to the cell surface, a central alpha helical domain (stalk) with high propensity to form coiled-coil structures, an N-terminal globular head that has been associated with binding to specific cellular receptors, and a signal peptide for secretion via the Sec pathway. This group includes well-known proteins, such as YadA of *Yersinia* spp. (Bliska *et al*., 1993a; Skurnik *et al*., 1994; Iriarte and Cornelis, 1996), UspAs proteins of *Moraxella catarrhalis* (Lafontaine *et al*., 2000; Hill and Virji, 2003), NadA of *Neisseria meningitidis* (Comanducci *et al*., 2002; Capecchi *et al*., 2005), Vomp proteins of *Bartonella quintana* (Zhang *et al*., 2004) and BadA of *B. henselae* (Riess *et al*., 2004). Canonical architecture of these proteins has been proposed in a well-known study (Hoiczyk *et al*., 2000) and in a recent function-structure work on UspA1 (Hill *et al*., 2005): here, the extracellular moiety, the passenger domain, consisting of the elongated stalk, neck and head, confers to the prototypic member of the family its characteristic drumstick appearance on the bacterial cell surface with the specific adhesive capabilities localized within the N-terminal globular head (Hoiczyk *et al*., 2000; Roggenkamp *et al*., 2003; Desvaux *et al*., 2004).

Proteins of the Oca family are often encoded by genes carried on mobile genetic elements**.** The YadA protein is not ubiquitous in *Yersinia* strains, as its coding gene is located on the pYV virulence plasmid, which is carried only by pathogenic *Yersinia* species (Cornelis *et al*., 1998; El Tahir, 2001).

Similarly, the *nadA* gene is present only in a subgroup of *N. meningitidis* strains belonging to hypervirulent meningococcal lineages and is characterized by a low GC content, suggesting gene acquisition by horizontal transfer (Comanducci *et al*., 2002).

Given the prominent role played by these molecules in the virulence of the related bacterium, in this study we conducted a search for Oca homologues in finished and unfinished bacterial genomes and identified a novel protein that we called HadA (Haemophilus adhesin A), from the invasive clone of *H. influenzae* biogroup *aegyptius* (Hae). Hae is classically associated with the Brazilian purpuric fever (BPF) disease, a fulminant and often fatal septicaemic infection of young children, first recognized in Brazil in 1984 (CDC, 1985; Brenner *et al*., 1988; Group, 1992), which typically follows episodes of purulent conjunctivitis (Harrison *et al*., 2008). All cases of BPF of Brazilian origin appear to be caused by a distinct lineage of closely similar but not identical strains of *H. influenzae*, hereafter referred to as the BPF clone. The BPF clone is phylogenetically closely related to *H. aegyptius*, an organism previously associated only with non-invasive purulent and contagious conjunctivitis. These observations suggest that BPF clones may possess special virulence factors able to transform bacteria involved in superficial infections into deadly pathogens. Various studies have been focused on this aspect, trying to identify determinants responsible for the invasive power of the BPF clone (Brenner *et al*., 1988; Weyant *et al*., 1990; Whitney and Farley, 1993).

In the present study, we identified HadA as a new TAA specific to the invasive clones of *H. influenzae* biogroup *aegyptius*. When expressed on the surface of *Escherichia coli*, HadA is assembled in trimers and mediates adhesion to and invasion into host cells. Structure analysis of the HadA extracellular domain revealed that is dissimilar from the canonical architecture described for Oca molecules.

Results

Identification of structural homologues to NadA

To identify members of the Oca family in other pathogens, we analysed *in silico* available bacterial genome sequences. The highest sequence similarity among known Oca proteins is restricted to the C-terminal translocation unit, which in NadA corresponds to the last 72 residues (Comanducci *et al*., 2002; Scarselli *et al*., 2006).

By using this NadA domain as query sequence to screen the non-redundant GenBank protein databank, and the databases of unfinished bacterial genomes we retrieved a number of hits, most of which had already been described by Hoiczyk *et al*. (2000).

To identify more distant members of this family, we subsequently used each of these proteins as a probe to perform further searches and retrieve additional hits, which were evaluated in terms of secondary structure analysis, coiled-coil prediction and presence/absence of a leader peptide. Despite the low sequence similarity displayed within the passenger domains, the majority of the identified proteins had a central coiled-coil and an N-terminal globular domain, recognized as the stalk and the receptor-binding domain respectively.

In addition to already known Oca proteins (Table S1), we identified a number of new putative members of the family (Table 1).

Most oligomeric coiled-coil adhesins, including YadA and NadA, are encoded on mobile genetic elements that are harboured by a subset of virulent strains. Therefore, it is reasonable to expect that newly identified NadA-like molecules could be specifically present in strains associated with virulence.

To test this hypothesis, we performed an additional search on selected GenBank entries, which include the

Table 1. New Oca proteins identified *in silico*. Only hits > 35% identity were reported.

Species	Protein ID	Length (aa)	% Identity to NadA anchor	Coiled-coil prediction	Leader peptide	G+C content (%)	*G*+C average (%)	Coded on a mobile element	Function characterized
Haemophilus influenzae biogroup *aegyptius*	HadA	256	84.6	Strong	Yes	35.1	38.2	Yes	Adhesin/invasin
Vibrio fischeri	VF2491	435	36.5	Weak	Yes	37.7			Hypothetical protein
Brucella abortus	Bruab1_1825	236	35.7	Strong	No	51.2			Hypothetical protein
Brucella suis 1330	BR1846	278	35	Strong	No				Hypothetical protein
Brucella melitensis 16M	BMEI0205	155	35	Strong	No				Immunoglobulin binding protein EibE
Mannheimia succiniciproducens MBEL55E	MS0748	5399	36	Strong	Yes				Hypothetical protein
Shigella flexneri 2a str. 301	SF3641	990	44	Strong	No	51.5			Autotransporter adhesin
Ralstonia eutropha JMP134	Raeut03004059	465	50	Strong	No				Autotransporter adhesin
Escherichia coli UPEC (CFT073)	c4424	1778	44	Weak	Yes	52.7	50.4%		Putative adhesin
Escherichia coli O157:H7	ECs4480	1588	44	Weak	Yes	50.3			Putative adhesin
Escherichia coli K1(RS218)[a]	ECK1	339	38	Strong	Yes	44[a]		Yes	Hypothetical protein
Escherichia coli EPEC (E2348/69)[b]	EPEC	339	38	Strong	Yes	48.3		Yes	Hypothetical protein
Escherichia coli EAEC (O42)[b]	EAEC	718	44	Strong	Yes	47.5	51.6	Yes	Hypothetical protein

a. This hit was identified using the Blast server available at the University of Wisconsin *E. coli* genome project web site (http://www.genome.wisc.edu/sequencing/rs218.htm).
b. These hits were identified using the Blast server available at the Sanger Institute Blast web site (http://www.sanger.ac.uk/Projects/Escherichia_Shigella). Coiled coil propensities were evaluated with Paircoil software available at the Expasy web server (http://www.expasy.org). Strong propensity was defined by scores higher than 0.7. Weak propensity was defined by scores between 0.5 and 0.6.

nucleotide sequences of clones derived from subtractive hybridization data between pathogenic and non-pathogenic strains.

By this analysis, we detected a 77% identity over the amino acid sequence within the 3′-end of a clone (AF416115) derived from a polymerase chain reaction (PCR)-based subtractive genome hybridization study performed between the BPF prototype strain F3031 and the non-invasive *H. aegyptius* F1947 isolate (Smoot *et al*., 2002). The clone has a length of 1151 bp and contains the partial 3′-end sequence of an ATP-dependent RNA helicase (*srmB*) gene followed by an intergenic region and the 5′-end sequence of a gene coding for the first 223 N-terminal residues of a protein sharing 36% identity with the meningococcal NadA adhesin.

Given this sequence similarity, we named the newly identified protein HadA (Haemophilus adhesin A).

hadA *is harboured on a genetic island present only in* H. influenzae *biogroup aegyptius*

The DNA sequence of the *hadA*-containing clone was checked against the genome of the *H. influenzae* rough type d (Rd) strain KW20. This strain was originally an encapsulated strain but lost its capsule production.

The 5′ region matched the *srmb* gene (*hi0422*), while both the intergenic and the partial *hadA* sequences were absent.

To define the *hadA* DNA region in the invasive F3031 strain of *H. influenzae* biogroup *aegyptius* (BPF clone), and get a global perspective on its arrangement in other *Haemophilus* taxa, we designed a pair of oligonucleotide primers mapped on conserved regions upstream and downstream of *hadA* sequence (the *srmb* and *hi0419* genes) and performed PCR analysis on the strains F3031, F1947 of *H. aegyptius*, NT36 of non-typeable *H. influenzae* (NTHi) and type b strain Eagan.

Sequencing of the amplified fragments revealed the complete organization of the corresponding region (Fig. 1A).

The *hadA* region in the BPF strain F3031 is 2159 bp long and includes the 771 bp *hadA* gene, flanked by regions harbouring predicted promoter and terminator sequences. Downstream of *hadA*, and on the reverse orientation, there are two additional open reading frames (ORFs), *orf1*, coding for a protein homologues to a histone acetyltransferase of *Histophilus (Haemophilus) somnus*, and *orf2*, which corresponds to the *hi0420* of the Rd genome (Figs 1A.i). The GC composition of the complete segment is 34.3%, significantly different from the average value of 38%, previously reported for the whole genome of *H. influenzae,* and therefore suggestive of a horizontal gene transfer. The F1947 strain has an organization almost identical to that of the Rd, which consists of

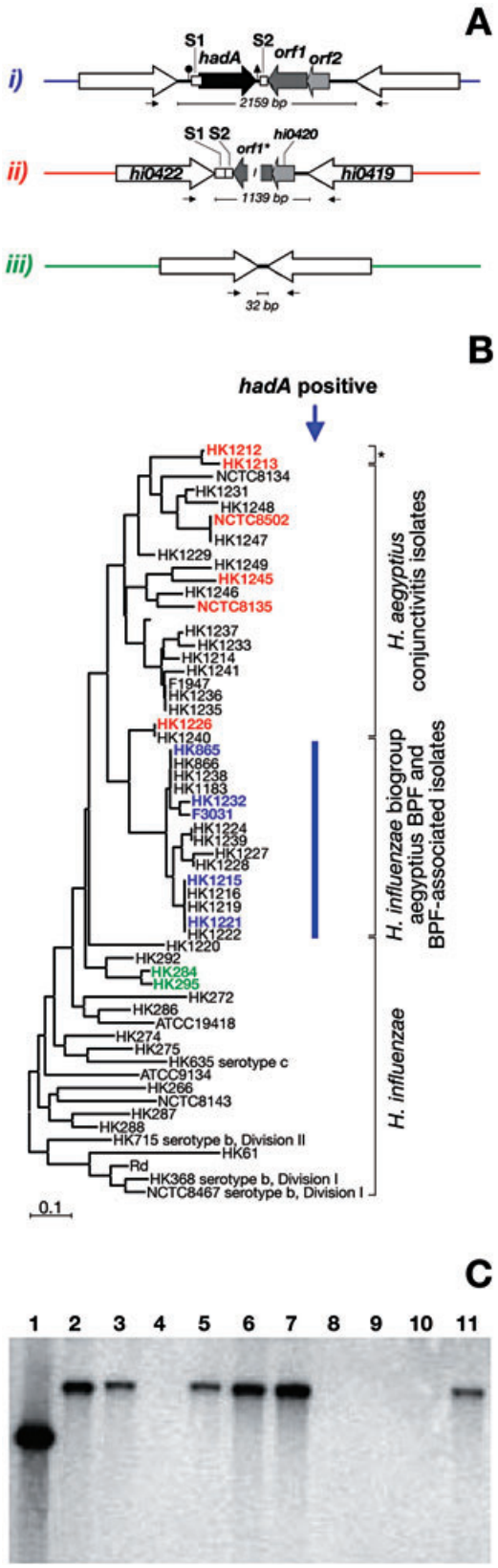

Fig. 1. (A) The *hadA* locus in *H. influenzae*. (i) Structure of the *hadA* region in BPF strain F3031. The flanking genes are white, while the genes belonging to the *hadA* region are in grey scale. The position of the *hadA* predicted promoter (filled circle) and terminator sequences (filled triangle) are shown. (ii) Remnants of the locus in *H. influenzae* Rd strain KW20 and in the non-invasive strain F1947 of *H. aegyptius*. Gene names derive from the *H. influenzae* Rd genome annotation. Asterisk (*) indicates that o*rf1* is frame-shifted here. (iii) The *hadA* region is completely absent from non-typeable *H. influenzae* strains 86-028NP (NC_007146.1), R2846 (NZ_AADO00000000), R2866 (NZ_AADP00000000), NT36, and from type b strain Eagan; in these strains the locus is substituted by a short stretch of 32 bases. S1 and S2 represent the location of short nucleotide segments remnant of recombination events. Arrows indicate the position of the forward and reverse primers used to amplify the locus in the various strains.
B. Presence of *hadA* gene in a panel of *H. influenzae* isolates. The presence of the gene has been evaluated by Southern blot analysis. The probe used was the full-length *hadA* gene from F3031 BPF strain. The original dendrogram was built on the basis of MLEE results (Kilian *et al*., 2002). Coloured names mark strains where the *hadA* locus has been sequenced. Strains having the same locus organization described for F3031, F1947 and NTHi are coloured in cyan, red and green respectively. Asterisk (*) indicates Australia isolates from BPF-like infectious.
C. Southern blot analysis. Genomic DNA from *H. influenzae* and *H. aegyptius* strains was purified, digested with XhoI and transferred to a nylon membrane, which was probed using the *hadA* gene from F3031 strain. The lanes show: (1) plasmid with *hadA* gene (positive control), (2) BPF strain HK1222, (3) BPF strain HK1221, (4) *H. influenzae* strain HK1220, (5) BPF strain HK1219, (6) BPF strain F3031, (7) BPF strain HK1215, (8) *H. aegyptius* strain HK1214, (9 and 10) Australian BPF-like isolates HK1213 and HK1212 respectively, and (11) BPF strain HK1183. This representative Southern blot illustrate that presence of the *hadA* gene was exclusively associated with Brazilian *H. influenzae* biogroup *aegyptius* isolates from or associated with BPF cases.

a segment of 1139 bp, encoding a frame-shifted form of *BPF-orf1,* and the *hi0420* homologue (Figs 1A.ii). In this case the GC composition is 32%. Finally, the NT36 NTHi and the type b *H. influenzae* strains completely lack the whole region (Figs 1A.iii).

These results indicate that the *hadA* gene is specific for the BPF F3031 strain and no counterpart is present in none of the other *H. influenzae* strains analysed.

We investigated the distribution of *hadA* by Southern blot analysis in a wider panel of strains representing various phylogenetic lineages of *H. influenzae*, including encapsulated and non-encapsulated (non-typeable) bacteria and clones of *H. influenzae* biogroup *aegyptius*, in addition to strains clustering with the type strain of *H. aegyptius.* As shown in Fig. 1B and C, only BPF-associated strains hybridized with the *hadA* probe.

Sequencing of the region in 12 strains selected as representative of this collection revealed the organization described in Fig. 1A: BPF isolates, positive in Southern blot, had the same organization as F3031 (i); strains not hybridizing with *hadA*, more closely related to *H. aegyptius*, including two Australian strains isolated from BPF-like disease, showed an arrangement of the region similar to that of F1947 (ii); strains phylogenetically closer to

NTHi had a structure comparable to Eagan (iii) (Fig. 1B). All loci were remarkably conserved relative to their prototypic sequences and the *hadA* gene was 100% identical when present.

Collectively, our data show a variable organization of the *hadA* region among *Haemophilus* strains, and particularly the absence of the *hadA* gene in non-BPF-associated strains.

HadA is an atypical surface trimeric coiled-coil autotransporter

The *hadA* gene product is a protein of 256 residues with a predicted leader peptide of 26 amino acids. Sequence similarity searches indicated that HadA has two very close homologues, the meningococcal adhesin/invasin NadA and the invasion-related protein of *Aggregatibacter (Actinobacillus) actinomycetemcomitans* ApiA (Li *et al*., 2004). Examination of the amino acid homology of HadA with NadA showed that the higher degree of sequence identity is restricted to the carboxy-terminal region (70% within the last 72 amino acids), while it drops below 28% along the rest of the protein. Despite the low level of primary structure similarity within the central domain, secondary structure predictions indicate a similar coiled-coil composition for the proteins consistent with the described Oca protein features. However, in contrast to NadA and ApiA, structural analysis of HadA indicates the presence of a continuous coiled-coil motif spanning the entire length of the putative passenger domain (amino acids 27–184) (Fig. S1). HadA is therefore predicted to lack the N-terminal domain commonly identified as globular head and typically associated with the receptor binding activity.

We further analysed the sequence of the NadA and HadA passenger domains using the MULTICOIL software. The structural organization of both NadA and HadA coiled-coil regions appears not to be uniform: regions with a propensity to form dimeric coiled-coils alternate with regions having a clear tendency to form trimeric coiled-coils (Fig. S2). Taking into account these different properties, we elaborated for the two proteins the models depicted in Fig. 2, where the trimeric coiled-coil results from inter-chain interactions while the dimeric coiled-coils are determined by intra-chain interactions. We hypothesized that in the case of HadA the dimeric coiled-coil protrusions form at the N-terminus of the stalk a functional domain, which mediates the binding capabilities of the protein.

To investigate whether the *hadA* gene is functional and actually encodes for a protein of the Oca family, we examined its expression in the BPF strains F3031 and HK1221 and in *H. influenzae* Rd (negative control). Immunoblot analysis of total protein extracts stained with a HadA-specific antibody revealed in both the BPF isolates specific immunoreactive proteins migrating to about 30 and 90 kDa, corresponding to the expected molecular weight of monomeric and trimeric HadA forms, respectively, which were absent in the Rd strain (Fig. 3A). Furthermore,

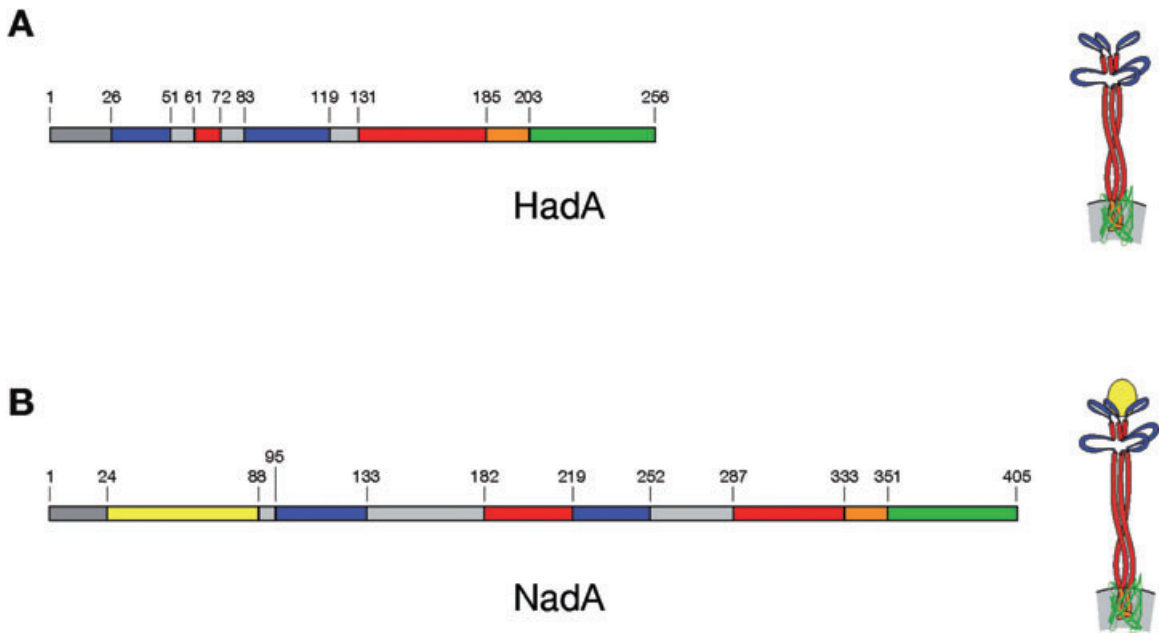

Fig. 2. HadA and NadA architectures. Proposed three-dimensional organization of HadA and NadA proteins. Portions of the extracellular passengers domain, which are predicted to form dimeric and trimeric coiled-coils are coloured in blue and red respectively. The NadA 'globular head' is coloured in yellow. The α-helix linker region (L2L1) and beta barrel parts within the integral outer membrane translocator domains are coloured in orange and green respectively.

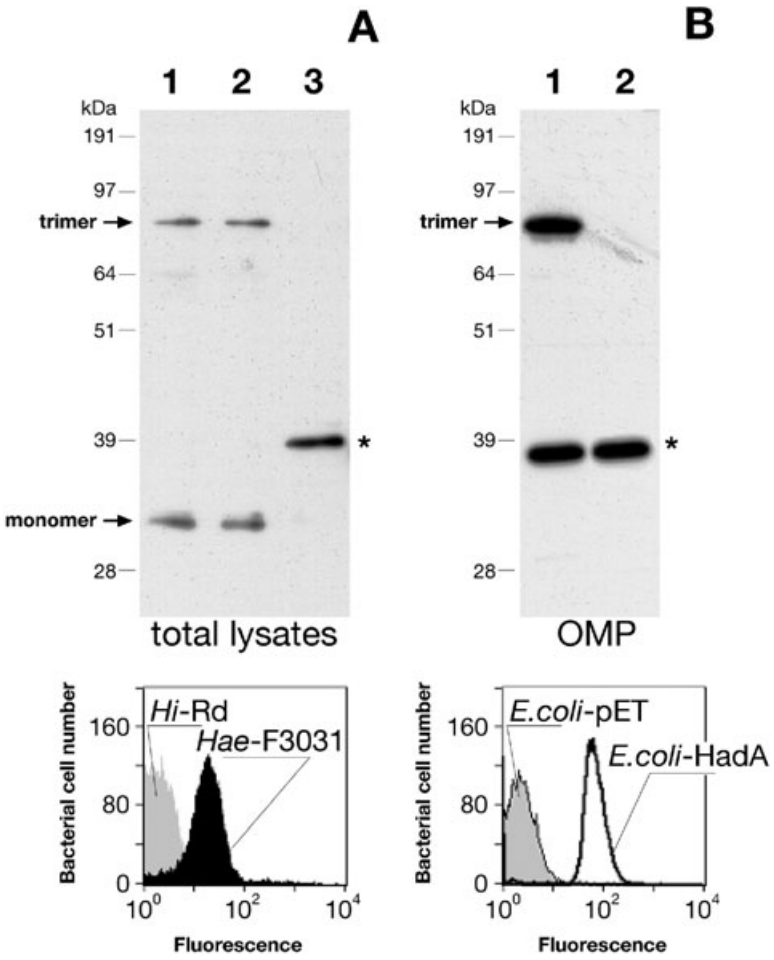

Fig. 3. HadA expression in BPF and *E. coli*.
A. Immunoblot analysis of total cell lysates from *H. influenzae* biogroup *aegyptius* (Hae: lane 1 strain F3031, lane 2 strain HK1221) and *H. influenzae* (Hi: lane 3 strain Rd); FACS analysis of HadA on whole-cell bacteria. Strain Rd was used as negative control and the corresponding histogram (grey-filled histogram) was superimposed on results with F3031 strain (black filled histogram).
B. Immunoblot analysis of outer membrane proteins (OMP) from *E. coli*-HadA (lane 1) and *E. coli*-pET (vector alone, negative control) (lane 2); asterisks indicate a non-specific cross-reactive band. FACS analysis of HadA on whole-cell bacteria. Strain *E. coli*-pET was used as negative control and the corresponding histogram (grey- filled histogram) was superimposed on results with *E. coli*-HadA strain (solid line). All the assays were performed using a rabbit serum anti-HadA-His as primary antibody.

FACS analysis on whole bacteria revealed a specific fluorescent shift associated with the BPF strain F3031 (Fig. 3A). To extend these results we generated a recombinant *E. coli* strain expressing HadA. SDS-PAGE and immunoblot analysis of total lysates from *E. coli*-HadA showed the presence of the two HadA bands, which were absent in *E. coli*-pET (vector alone, negative control) (not shown). Immunoblot analysis of outer membrane proteins from *E. coli*-HadA revealed that only the trimeric form was detected in the outer membrane (Fig. 3B). Additionally, FACS analysis confirmed the presence of HadA exposed on the *E. coli* surface (Fig. 3B).

To further study the structural organization of the extracellular domain of HadA, we analysed the conformation of the protein expressed on the *E. coli* outer membrane vesicles (OMV) surface by Cryo-electron microscopy and single-particle approach. The cryo preparation showed different sized OMV particles with a homogeneous distribution of short antenna-like appendages protruding from the *E. coli*-HadA OMV, which were absent in the *E. coli*-pET OMV (Fig. 4).

The antenna-like appendages appear as short faint structures with lengths varying from 5 up to 6 nm and an average width of ~6 nm. From digitized micrographs of OMV only 40 HadA spikes could be manually selected and boxed into 64×64 pixel frames due to the background noise and the small size of the spikes. All the single HadA spikes boxed were processed by first centring and aligning them both rotationally and translationally. All spikes that did not align were eliminated. Finally, all the 10 images were kept and used to generate averaged HadA spikes with an increased signal-to-noise ratio. The resultant 2D averaged image shows HadA as a trimer with a clover-like appearance, where the elongated stalk is laterally decorated by important protruding densities (Fig. 5). This is in agreement with the *in silico* prediction, in which the extracellular portion of HadA is an elongated coiled-coil trimeric stalk ending with a clover-like structure, which we hypothesize to be formed by the lateral dimeric coiled-coil protrusions (Fig. 2).

To further support this model, we performed the same structural analysis on OMV of *E. coli* expressing NadA, the *N. meningitidis* homologue which possess a typical N-terminal globular head (Capecchi *et al*., 2005). Two hundreds NadA images were boxed into 64×64 pixel frames and classified into 8 class averages. In the case

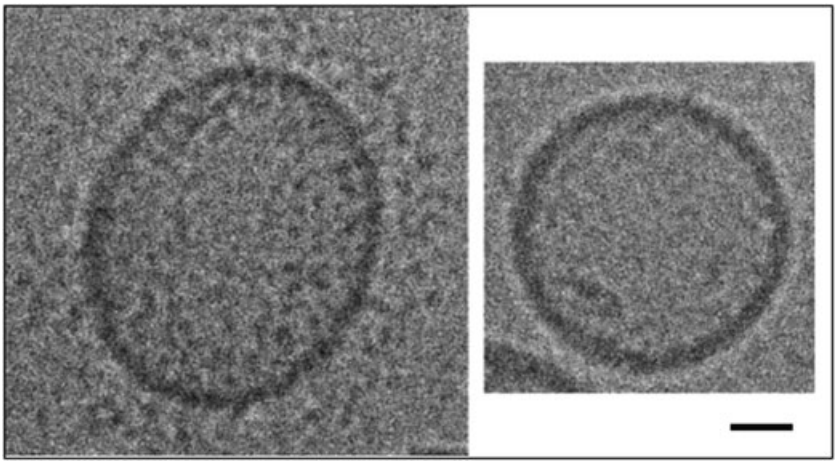

Fig. 4. Cryo-electron microscopy images of *E. coli* OMV. Micrographs of OMV from *E. coli*-HadA (left panel) and *E. coli*-pET (right panel). Scale bars correspond to 100 nm. Both images were taken at 50000× magnification.

of NadA, the protein showed the typical drum-stick organization with a globular head more clearly defined. The two molecules share similar structure in the stalk region with just a subtle difference in length, with the NadA stalk l0 Å longer than the HadA stalk (Fig. 5).

The comparison of the NadA and HadA set of data is fully supporting the models where the presence of the clover-like domain, which alone constitutes the HadA head, can be predicted also within the NadA sequence. The compact and globular head observed in this case could likely be constituted by the amino acid residues of the dimeric protrusions and the remaining N-terminal residues of the protein.

The presence of the apparently larger tip of HadA could be justified by the high flexibility of the three long apical loops that in absence of a head assume different orientations on the plane of projection generating a diffuse large density at the tip of the structure. On the contrary, the averaged NadA head results to be more defined and compact due to the presence of the loops that are closely associated to each other and to the head itself.

Collectively, these results show that HadA is a novel and atypical trimeric autotransporter exposed to the bacterial surface.

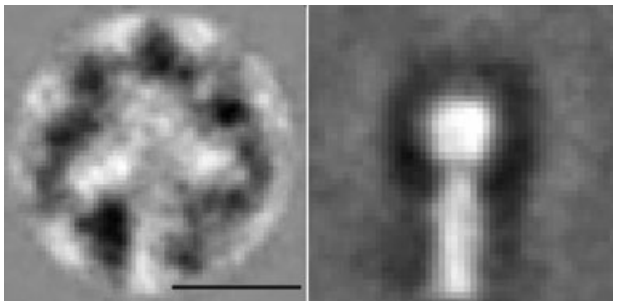

Fig. 5. Representative class averages of HadA (left panel) and NadA (right panel). The images show HadA as a trimer with a clover-like appearance where the elongated stalk is laterally decorated by three important protruding densities. On contrary, NadA protein shows the typical drum-stick organization with a globular head clearly defined. The density disorder observed in the HadA head is due to the three apical loops that, being flexible structures, are projecting in different direction onto the imaging plane generating a wider and less compact head. The NadA head compactness is probably due to the tightness of the three NadA apical loops to the NadA head. Scale bars correspond to 50 Å.

HadA promotes bacterial aggregation

Growing in liquid culture *E. coli*-HadA, we noticed the presence of bacterial aggregates, clearly visible at the bottom of the tube. Phase-contrast microscopy analysis showed that they had a 'cloud-like' appearance (Fig. 6A). To quantify this phenomenon and to investigate whether the ability to form aggregates is dependent upon HadA–HadA homologous recognition or rather upon the interaction of HadA molecules with *E. coli* membrane structures, we performed tube-settling assays with cultures of *E. coli*-HadA and *E. coli*-pET strains. Bacteria were grown to stationary phase, then different tubes were prepared, diluting the bacterial cultures to an optical density (OD) of 1: (i) only *E. coli*-pET, (ii) only *E. coli*-HadA, and (iii) a mixture of equivalent amounts of *E. coli*-pET and *E. coli*-HadA. The OD of the three cultures was measured over time and the results are reported in Fig. 6B. While the OD of the *E. coli*-pET culture remains almost stable over time, we observed a remarkable OD decrease of the cultures containing only *E. coli* expressing HadA. Interestingly, the OD observed for cultures containing equivalent amounts of *E. coli*-pET and *E. coli*-HadA was intermediate. These results suggest that the clumping phenotype is driven by a mechanism of HadA–HadA homophilic interaction, although the exact mechanism of this phenomenon remains unknown.

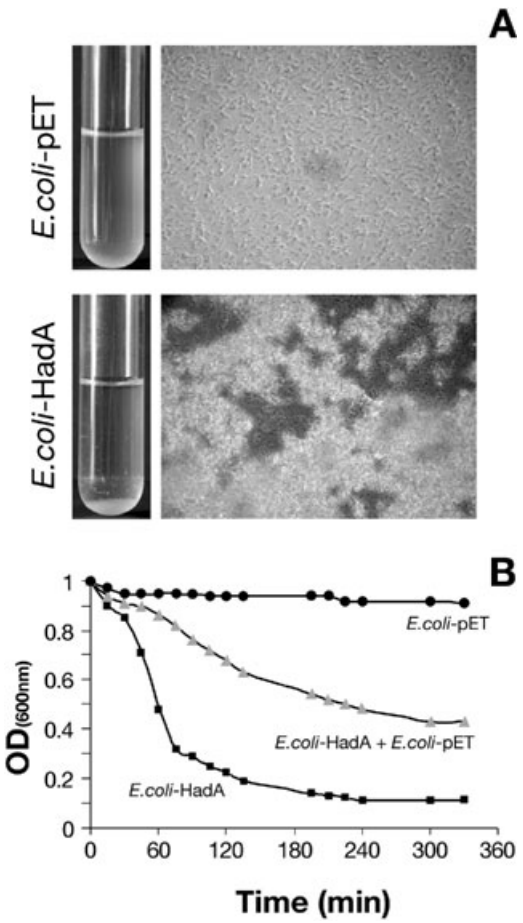

Fig. 6. HadA promotes *E. coli* aggregation.
A. Tube-settling experiment of stationary phase cultures of *E. coli*-pET and *E. coli*-HadA after incubation at room temperature for 5 h. Phase-contrast micrographs of *E. coli* cultures showing the presence of bacterial aggregates in *E. coli*-HadA, compared with *E. coli*-pET.
B. Bacterial aggregation of the different bacterial cultures was quantified by measuring the decrease of absorbance at 600 nm over time.

HadA mediates bacterial adhesion, invasion and microcolony formation

Because of the similarity of HadA to TAAs, we investigated its ability to mediate *in vitro* bacterial adherence and invasion of Chang epithelial cells (human conjunctival cells), which represent an *in vitro* model to study infection of *H. influenzae* biogroup *aegyptius* (St Geme *et al*., 1991; Farley *et al*., 1992). In accordance with previous observations (Li *et al*., 2003), we found *H. influenzae* biogroup *aegyptius* strains resistant to genetic manipulation, and our attempts to construct an isogenic BPF *hadA* mutant were unsuccessful, also following a previously described method (Segada and Lesse, 1997). Hence, we decided to carry out our analysis with the non-pathogenic and non-invasive *E. coli* strain expressing HadA, which permitted us to focus exclusively on the potential role of HadA in virulence.

Chang cell monolayers were infected with *E. coli*-HadA and *E. coli*-pET and cell-associated bacteria were calculated by plating cell lysates. As shown in Fig. 7A, a > 200-fold increase for *E. coli*-HadA with respect to *E. coli*-pET was observed.

Thus, HadA has the ability to promote adhesion. This potentially important function was further analysed examining the capability of the anti-HadA antibody to block attachment of bacteria to the cells. Pre-incubation of *E. coli*-HadA with increasing concentrations of anti-HadA serum resulted in a significant dose-dependent decrease in adherence (Fig. 7B). In order to prove the adhesive role of HadA in the native background of BPF-associated bacteria (without the possibility of deleting the *hadA* gene), we performed the same experiment trying to inhibit the adherence of the *hadA* positive F3031 strain to Chang cells. As shown in Fig. 7C, we observed approximately a 50% reduction mediated by the anti-HadA antibody, while a preimmune sera did not impair the adhesive capability. Considering that bacterial adhesion is a multifactorial process, and that it is almost certainly that HadA is not the only protein able to mediate adhesion of the BPF strains to Chang cells, we believe that this level of reduction is significant and demonstrates a role of HadA in the BPF bacteria adherence.

We explored whether HadA is also able to promote entry of *E. coli* into epithelial cells. A Chang monolayer was infected with the same strains and invasion was measured using a gentamicin invasion assay. As shown in Fig. 7A the presence of HadA induces more than one-log increase in the number of intracellular bacteria.

Further analysis by scanning electron microscopy (SEM) clearly showed the presence of large microcolonies of *E. coli*-HadA associated with the Chang cell membrane (Fig. 8A–C). Transmission electron microscopy (TEM) analysis confirmed the close association of bacteria with the cell surface and the formation of membrane protrusions around adherent bacteria (Fig. 8D). Moreover, immunoelectron microscopy revealed staining of HadA on the bacterial surface in the junction between bacterial and epithelial cell membranes, between interacting bacteria and in intracellular bacteria (Fig. 8E and F).

Previous studies reported that BPF-associated strains attach, invade and multiply intracellularly in a HMEC-1 endothelial cell line (Quinn *et al*., 1995).

We tested whether the *E. coli*-HadA strain interacts with human umbilical vein endothelial cells (HUVECs) and found that HadA is also able to mediate bacterial adhesion to and invasion of these cells (Fig. 7D).

Finally, we evaluated whether HadA is able to bind to ECM. We quantified HadA-mediated adherence to selected proteins of ECM in an *in vitro* adherence assay

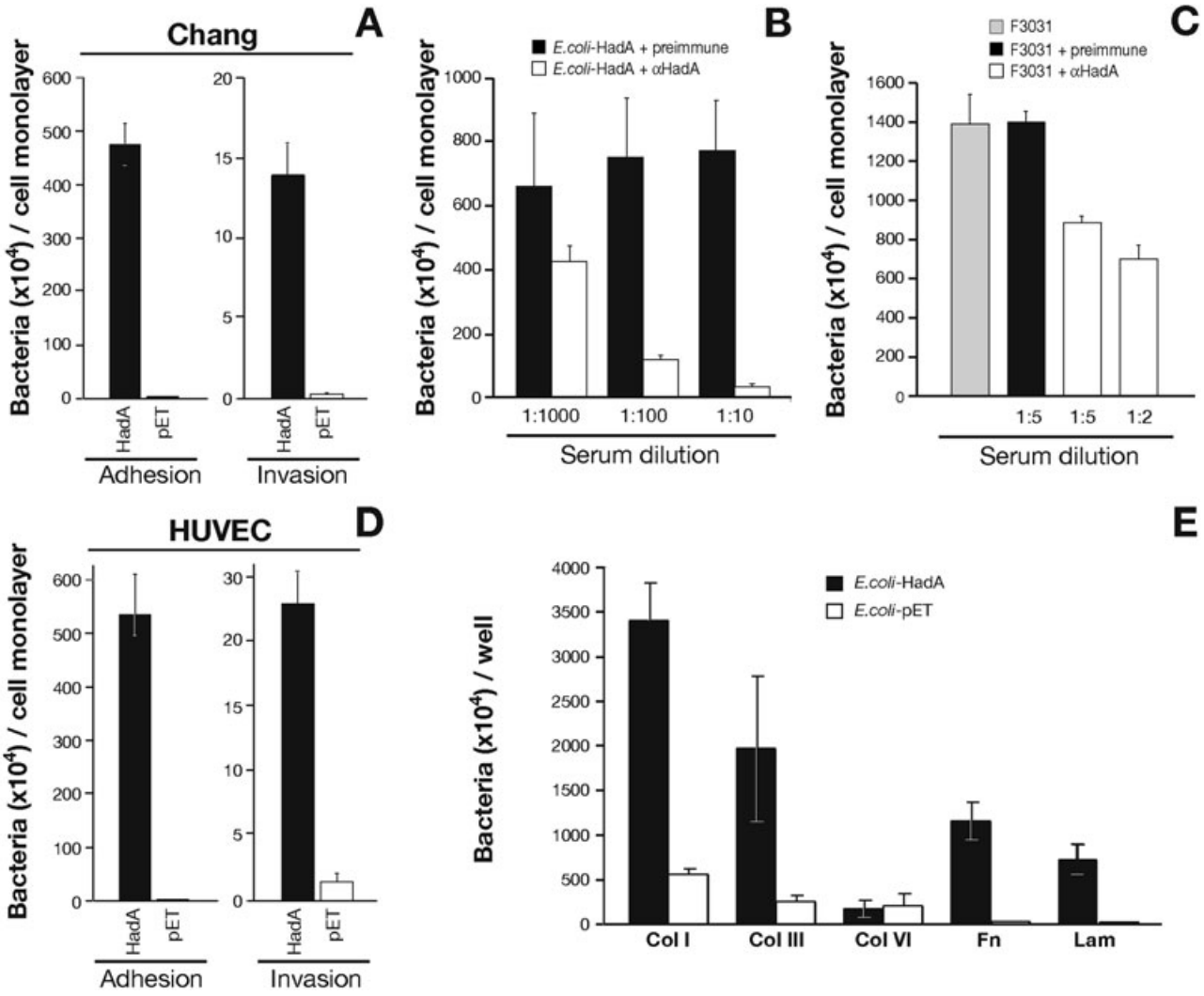

Fig. 7. Role of HadA in cell adhesion and invasion.
A. Adherence to and invasion into Chang epithelial cells by *E. coli*-HadA (black bar) compared with *E. coli*-pET (white bar). Adherence was calculated by counting the number of associated bacteria on cell monolayers. Invasion was calculated by counting the number of intracellular bacteria after gentamicin treatment.
B and C. Inhibition of epithelial cell adhesion by anti-HadA serum. (B) Adherence of *E. coli*-HadA to Chang cells was inhibited by increasing concentrations of anti-HadA antibodies. Treatment with a preimmune rabbit serum diluted at the same concentrations had no effect on adherence. (C) Adherence of *H. influenzae* biogroup *aegyptius* strain F3031 and inhibition by increasing concentrations of the anti-HadA antibodies. Treatment with the preimmune rabbit serum (diluted at 1:5) had no effect on adherence. The reduction in adhesion was not due to antibody-mediated bacterial clumping as demonstrated by light microscopy analysis (data not shown).
D. Adherence to and invasion into HUVEC cells by *E. coli*-HadA (black bar) compared with *E. coli*-pET (white bar). All the experiments were performed using an moi of approximately 1:100. Values represent the mean ± standard deviation of a representative experiment performed in triplicate.
E. HadA-mediated adherence to ECM proteins. Adherence to proteins of ECM by *E. coli*-HadA (black bars) and *E. coli*-pET (white bars). Adherence is expressed as cfu per well and values represent the mean ± standard deviation of a representative experiment performed in triplicate.

using plates coated with purified collagens I, III, VI, fibronectin and laminin. As shown in Fig. 7E, *E. coli*-HadA adhered significantly to collagens I and III, to a lower extent to fibronectin or laminin whereas no adherence to collagen VI was observed.

The data presented here show that HadA is a multifactorial adhesin, which is capable also to promote bacterial entry.

HadA binding domain: role of the N-terminal region and KGD motif

HadA lacks the typical N-terminal globular domain responsible for adhesiveness of many members of the Oca family. We hypothesized that the dimeric loops at the N-terminus of the HadA stalk form the functional domain directly involved in adhesion and invasion.

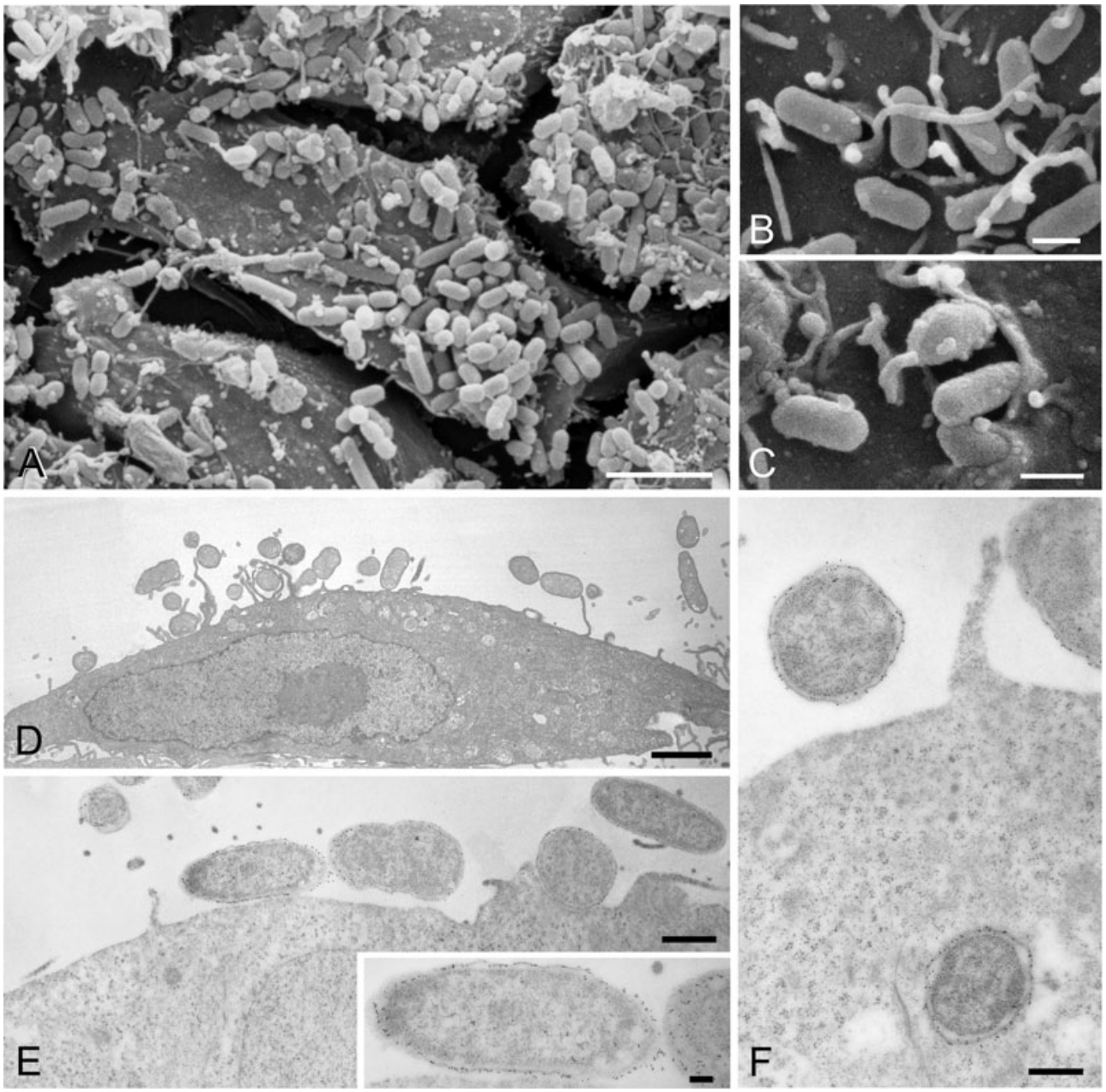

Fig. 8. Electromicroscopy analysis showing adhesion, invasion and microcolony formation of *E. coli*-HadA on the Chang conjunctival cell surface.
A–C. SEM analysis (Scale bars: 5, 1 and 1 μm respectively).
D. TEM analysis (Scale bar: 2 μm).
E and F. Immunogold labelling of *E. coli*-HadA using the anti-HadA antibody (Scale bars: 1 and 0.5 μm respectively). Inset in (E): magnification of the interaction between two *E. coli*-HadA bacteria.

This hypothesis was supported by the presence of the putative adhesive sequence motif $_{96}$KGD$_{98}$ included in one of the putative dimeric arms.

To assess this hypothesis we evaluated the stability and adhesive/invasive phenotypes of a series of *E. coli*-HadA mutants carrying different deletions along the putative N-terminal binding domain.

As reported in Fig. 9A, none of the deletions affected expression, trimer formation and surface localization of HadA. Interestingly, all the mutants except one did loose both the aggregative and the adhesion/invasion properties (Fig. 9B); in particular, HadAΔ49-69 mutant seems to have an increased capability to adhere to and invade Chang cells compared with the wild-type HadA (Fig. 9B).

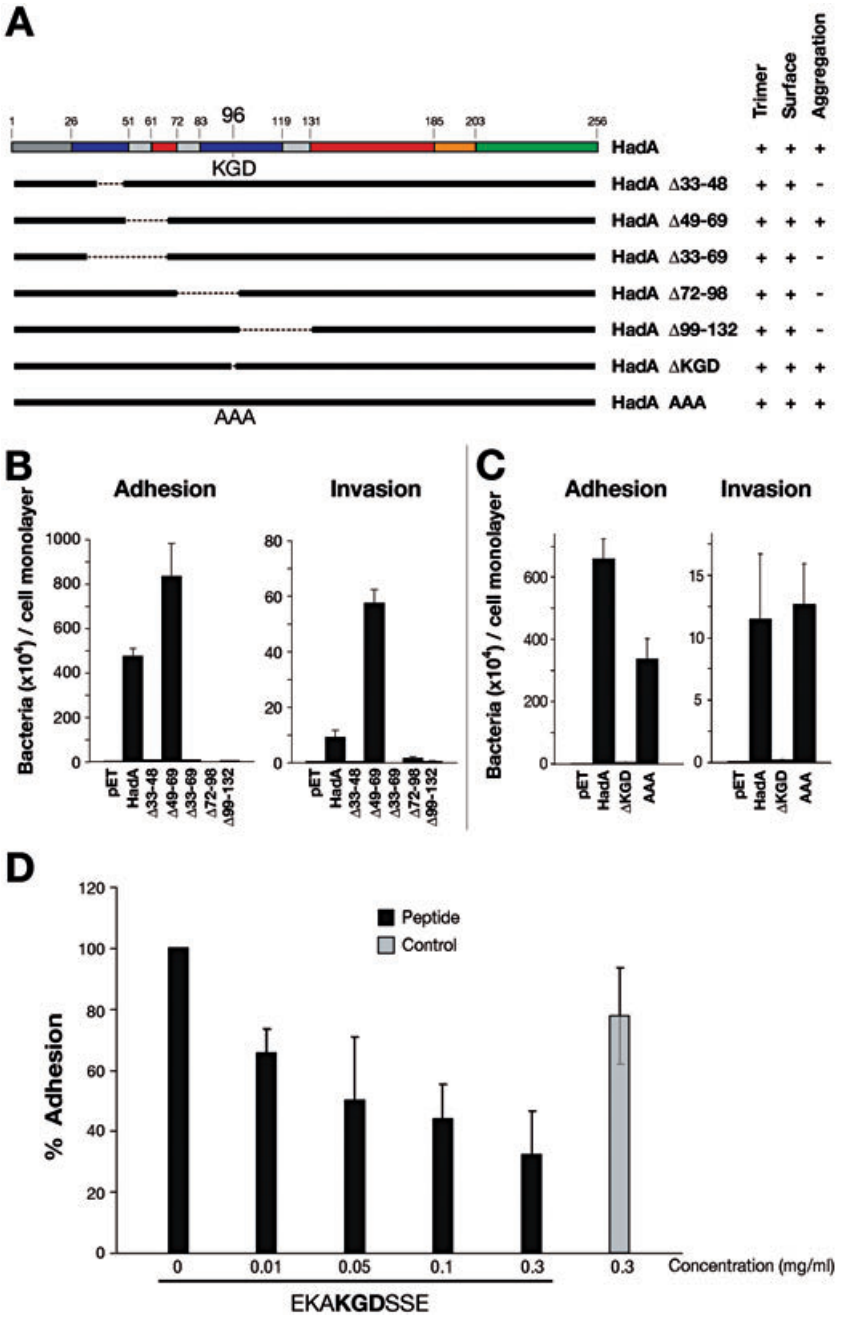

Fig. 9. Analysis of HadA binding region.
A. Schematic representation of the various HadA mutants used in this study. The leader peptide, the dimeric and trimeric coiled-coils, the α-helix linker and the beta region are indicated in colours according to Fig. 2. The phenotypes of trimer formation, surface localization and bacterial aggregation are indicated with a '+' (behaviour is like *E. coli*-HadA) or a '–' (behaviour is like *E. coli*-pET).
B and C. Adhesion and invasion of HadA mutants. Results are reported as cfu ($\times 10^4$) per cell monolayer and values represent the mean ± standard deviation of a representative experiment performed in triplicate.
D. A synthetic KGD containing peptide inhibits adhesion of *E. coli*-HadA. Chang cells were pre-incubated with a range of EKAKGDSSE peptide (0.01–0.3 mg ml^{-1}) or with a control peptide (C at 0.3 mg ml^{-1}) and the level of attachment was determined by a viable count assay.

From this analysis we conclude that all these deletions significantly altered the HadA N-terminal domain and consequently the functionality of the binding site to epithelial cells.

To test whether the KGD motif might be involved in HadA-mediated binding, two mutants were generated in *E. coli*: the first was a deletion mutant of the KGD sequence (named HadAΔKGD) and the second consisted of a triple mutant in which each amino acid of the KGD triad was substituted with an alanine residue (named HadA-AAA). Both mutants did not affect expression, trimerization and surface exposure of HadA (data not shown). Interestingly, the *E. coli* strain expressing HadAΔKGD showed a significant reduction in adherence and invasion of Chang epithelial cells (Fig. 9C). However, the triple mutant showed only a modest reduction in adhesion and no reduction in invasion of Chang cells (Fig. 9C). Subsequently, we generated mutants containing single-residue substitutions of the KGD motif into alanine, named HadA-AGD, HadA-KAD and HadA-KGA. While the HadA-KAD and HadA-KGA mutants behaved as the wild-type HadA, on the contrary, the HadA-AGD mutation caused a reduction in the adhesive pheno-

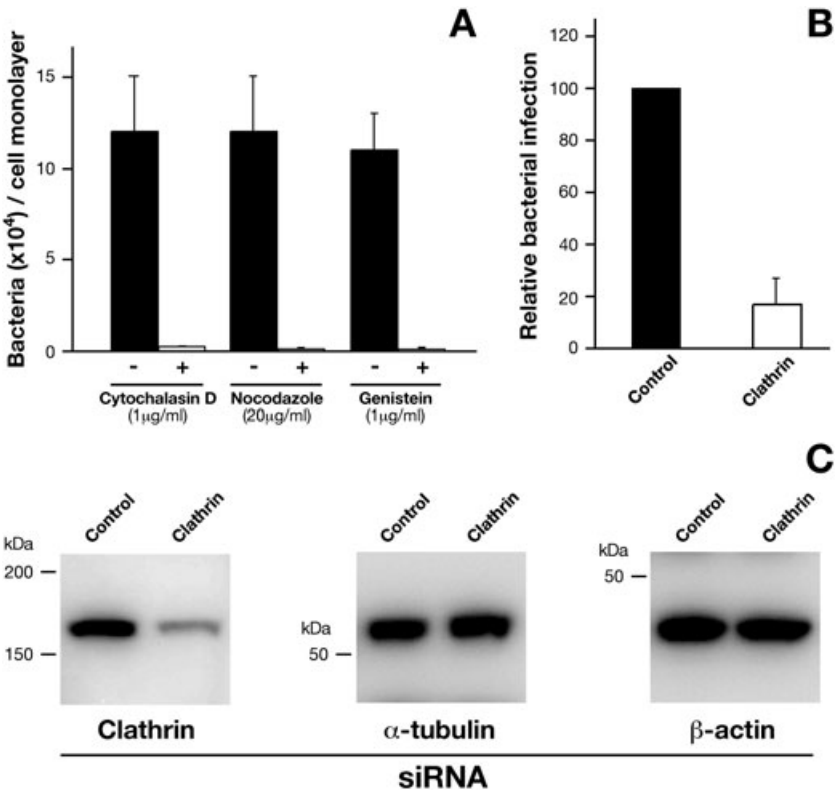

Fig. 10. Influence of cytoskeleton remodelling and clathrin in bacterial entry.
A. Effects of various inhibitors (Cytochalasin D, Nocodazole and Genistein) on Chang cell invasion by *E. coli*-HadA. Values represent the mean ± standard deviation of a representative experiment performed in triplicate.
B. Chang cells KD for clathrin were infected with *E. coli*-HadA. Colony-forming unit counts obtained from siRNA-pretreated cells were normalized to control siRNA (RNA not targeting any cellular mRNA)-treated cells (sixfold reduction, $P < 0.005$).
C. Protein KD by siRNA was tested by Western blot. The left lane corresponds to the control cells and the right lane corresponds to the cells treated with siRNA against clathrin. Actin and tubulin are shown as control.

type comparable to the triple mutant, indicating a different contribution of the single residues. All the three mutant strains showed an invasive capability comparable to the wild-type HadA (data not shown).

In order to evaluate with a different approach the role of the KGD sequence in adhesion, we measured the adherence of *E. coli*-HadA in the presence of a nonameric peptide containing the KGD triad and comprising residues 93–101 of HadA (EKAKGDSSE). This peptide inhibited the *E. coli*-HadA adhesion in a dose-dependent manner. No such inhibition was observed with a control peptide not containing the KGD triad (Fig. 9D).

Taken together, these data support the role of the KGD sequence in HadA-mediated adhesion and highlight the importance of the N-terminal domain of HadA in the interaction with epithelial cells.

Influence of cytoskeleton remodelling and clathrin in HadA-mediated entry

A deeper examination of the SEM analysis shows that *E. coli*-HadA induce membrane extension that zip around and engulf entering bacteria (Fig. 8B and C). This is reminiscent of the invasion process mediated by zippering bacteria that, interacting with cellular receptors, initiate a signalling cascade that results in actin polymerization and cellular membrane remodelling (Veiga and Cossart, 2006).

To address the invasion mechanism mediated by HadA, first we evaluated the role of cytoskeletal and tyrosine protein kinase inhibitors reported to block cell invasion by various pathogenic bacteria (Rosenshine *et al*., 1992a,b; Bliska *et al*., 1993b). Chang cells were pretreated with the microfilament inhibitor Cytochalasin D, with the microtubule inhibitor Nocodazole, and with the tyrosine protein kinase inhibitor Genistein before infection with *E. coli*-HadA. The results indicate that all three inhibitors drastically reduce bacterial invasion, suggesting that a signalling cascade and actin polymerization has to occur after HadA interaction (Fig. 10A).

It has been recently reported that zippering bacterial pathogens recruit clathrin for invasion of non-phagocytic cells (Veiga and Cossart, 2005; Veiga *et al*., 2007). To further clarify the HadA invasion process we evaluated whether it exploits a clathrin-dependent mechanism. We analysed bacterial entry into Chang epithelial cells in which expression of clathrin was knocked-down (KD) by siRNA. Cells in which clathrin expression was reduced were infected with *E. coli*-HadA and intracellular bacteria were counted after gentamicin treatment. As shown in Fig. 10B, a sixfold decrease was observed in clathrin-KD cells compared with control cells. Clathrin KD by siRNA was tested by Western blot, and actin and tubulin were used as controls (Fig. 10C). However, by immunoflorescence microscopy we did not observe a clear colocalization of

clathrin and bacteria at the entry site (data not shown), suggesting that the influence of clathrin in the invasion mechanism is not a result of a direct interaction with HadA.

These results confirm a role of HadA as a new invasin of the Oca family and suggest that HadA-dependent entry differs from that described for other zippering bacteria.

Discussion

Due to the marked sequence variability that characterizes the extracellular domains of the Oca family members, the automated retrieval of Oca is challenging. Recently, a bioinformatic tool to accomplish this goal has been presented by Szczesny and Lupas (2008), based on the identification of sequence motifs typical of this class of proteins. However, as the numbers of Oca members increases, it becomes clear that the existence of non-canonical proteins, lacking of some of Oca diagnostic features, could make difficult their identification.

This study initiated with an extensive *in silico* analysis, which led to the discovery of HadA, exclusively present and conserved in all lineages of *H. influenzae* biogroup *aegyptius* associated with the BPF disease, but absent in all the other *H. influenzae* and *H. aegyptius* strains tested.

Here functional studies showed that HadA is a trimeric autotransporter expressed by BPF isolates, that, when expressed on the surface of a non-invasive *E. coli* strain, was able to trimerize and induce massive bacterial adherence to Chang conjunctival epithelial cells and binding to laminin, fibronectin and collagen types I and III of the ECM.

Attachment to epithelial cells of the conjunctiva is a preliminary step in the pathogenesis of BPF caused by *H. influenzae* biogroup *aegyptius*. Enhanced attachment to conjunctival cells was demonstrated for BPF clone strain F3031 compared with that of a non-BPF strain, but the reason for this difference remains unknown (Farley *et al*., 1992). Moreover, *in vitro* adherence of *H. influenzae* biogroup *aegyptius* to conjunctival cells occurred independently of the presence of long pili detected in some strains (St Geme *et al*., 1991) and of the Hap protein, which is not expressed in BPF clone strains (Kilian *et al*., 2002), suggesting that other adhesive factors have to be present on the bacterial surface.

It is certain that several pathogenic bacteria possess a repertoire of adhesins that are called upon during their life cycle. We suggest that together with pilus and non-pilus adhesins, differentially expressed by *H. influenzae* biogroup *aegyptius*, HadA might play a role in the attachment of bacteria to human conjunctival cells during the initial stage of BPF disease, allowing enhanced colonization. We provide evidence that adherence of a BPF (*hadA* positive) strain to cultured conjunctival cells is inhibited by specific anti-HadA antibodies, suggesting that *in vivo* the presence of antibodies against HadA might prevent HadA-positive *H. influenzae* biogroup *aegyptius* strains from adhering to human cells.

It is noteworthy that collagen types I and III and laminin are all components of the basement membrane underlying the conjunctival epithelium (Abu el-Asrar *et al*., 1998; Abu El-Asrar *et al*., 2003). Fibronectin is also present on the surface of epithelial cells. In contrast to the situation with collagen types I and III, HadA does not bind collagen type VI, which is found mainly in cartilage. Moreover, as conjunctival inflammation results in increased production of collagens I and III and laminin, adherence to ECM, could contribute to the initial colonization as well as contiguous spread.

Like other autotransporters (Hasman *et al*., 1999; Sherlock *et al*., 2004; Zhang *et al*., 2004; Sherlock *et al*., 2005; Klemm *et al*., 2006), HadA has the intrinsic property to promote bacterial aggregation when expressed by *E. coli* and the formation of large bacterial microcolonies on the surface of infected cells, likely through interbacterial interactions due to HadA-HadA homophilic contacts. Autoaggregation is known for some virulence proteins and is usually accompanied by increased adherence and colonization with implications for bacterial pathogenesis, as it is of fundamental importance in the development of bacterial communities, such as microcolonies or biofilms (Ochiai *et al*., 1993).

In the case of *H. influenzae* biogroup *aegyptius*, the colonization pattern appeared to be as microcolonies on Chang epithelial cells (Kilian *et al*., 2002). The HadA protein might be in part responsible for this behaviour although the available evidence suggests that this phenotype is multifactorial as strains of *H. aegyptius*, which lacks HadA, also forms microcolonies on conjunctival cells (Kilian *et al*., 2002).

Escherichia coli expressing HadA also invades non-phagocytic cells. Electron microscopy analysis revealed the presence of membrane protrusions at the bacteria contact site, and around the bacteria, which are likely the results of host-signalling events induced by HadA. Indeed, we showed that the bacterial entry is associated with protein phosphorylation and cytoskeletal re-arrangements, key events of the invasion process mediated by zippering invasive bacteria. Signalling cascades promotes at the entry sites actin polymerization that allows the cellular membrane to remodel and engulf the entering bacteria (Cossart and Sansonetti, 2004).

It was commonly assumed that bacteria enter into host cells by mechanisms independent of clathrin-mediated endocytosis. However, recent studies have highlighted a role for clathrin in *Listeria* InlB-mediated actin polymerization and entry, revealing a new function for this endocytic protein in bacterial-induced internalization. Moreover,

clathrin-mediated endocytosis machinery is also widely used for entry of other bacterial pathogens that enter by a 'zipper' mechanism, such as *Yersinia pseudotuberculosis* and *Staphylococcus aureus* (Veiga *et al*., 2007). In the present study, we investigated the role of clathrin in the internalization of HadA expressing bacteria. HadA-dependent entry into epithelial cells was impaired in clathrin siRNA KD cells, but recruitment of clathrin to sites of bacterial interaction with the host cell was not clearly observed, suggesting, contrary to that observed in other bacterial infections, an indirect role for clathrin in the internalization process induced by HadA. The mechanism by which HadA expressing bacteria use clathrin to enter host cells remains unknown and will be evaluated in further studies.

The mechanism and the role of invasion in the pathogenesis of BPF are poorly understood. Although invasion of *in vitro* cultured epithelial cells by BPF bacteria seems to be occasional and strain-dependent (St Geme *et al*., 1991; Farley *et al*., 1992; Li *et al*., 2003), it is likely to play an important role during BPF disease. Entry of conjunctival cells may serve as an immune escape purpose in addition to facilitating penetration of the epithelial barrier to reach the bloodstream leading to systemic disease.

Finally, we show that HadA promotes adhesion and invasion by *E. coli* of HUVECs. This is in accordance with previously published data on adherence, invasion and intracellular multiplication observed with BPF strains, using a HMEC-1 endothelial cell line (Quinn *et al*., 1995). Thus, HadA is capable of multivalent interactions potentially related to BPF pathogenesis. Further work will be necessary to assess the function of HadA in the native context of *H. influenzae* biogroup *aegyptius*, although this might be difficult to achieve because this bacterium is averse to genetic manipulation, as also demonstrated by our unsuccessfully attempts in generating a HadA deletion mutant.

HadA is an unusual member of the Oca family, lacking the N-terminal 'globular head' detected so far among members of the Oca family. Nevertheless, HadA mediates adhesion to and invasion of host cells. By analysing the coil propensity profile of HadA protein, we predicted an alternative structure for the stalk, where the trimeric coiled-coil backbone is equipped with dimeric coiled-coil arms, each resulting from intra-chain interactions. We postulate that these lateral protrusions may constitute the adhesive domain, functionally corresponding to the 'globular head'. This model was confirmed by Cryo-electron microscopy analysis of *E. coli*-HadA, showing a clover-like structure for trimeric HadA passenger domain. In the case of NadA, the protein showed the typical drum-stick organization with a globular head clearly defined.

We used the model of the HadA passenger domain as a guideline to generate deletions in the N-terminal region, and demonstrated in all the mutants the simultaneous loss of aggregative and adhesion/invasion capabilities, which suggests a destruction of the overall structure of the HadA binding site. The mutant HadAΔ49-69, showing an increased capability to adhere to and invade Chang cells compared with the wild-type, represents the only exception. We speculate that this deletion caused a conformational change in the HadA structure that brings the trimeric molecule into a more favourable conformation for attachment and invasion.

It is known that the RGD motif present in molecules expressed by different microorganisms could serve as recognition site for integrins (Relman *et al*., 1990; Frankel *et al*., 1996). It has been reported that also the KGD motif is able to mediate interaction with integrins (Nykvist *et al*., 2001).

We hypothesized an adhesive function for the KGD motif, which, accordingly with the proposed model, is located in one of the predicted dimeric coiled-coil protrusions. This is supported by the finding that deletion of the KGD triad, as well as inhibition with a KGD containing peptide, caused a significant reduction in adherence. Moreover, KGD deletion affected bacterial invasion. However, mutagenesis of KGD in AAA impaired only the adhesion phenotype but not to the same extent as the deletion mutant. These data suggest a role of the KGD motif in promoting an effective binding, most probably in combination with other residues that may determine a more complex functional conformation. The exact contribution of the KGD motif in the HadA binding domain as well as its interaction with integrins needs further investigations.

In conclusion, as a unique member of Oca proteins, HadA provides novel mechanism of bacteria–host interaction and constitutes a valuable model for studying the other components of this broad family of highly versatile virulence factors that play multiple roles in bacterial pathogenesis.

Experimental procedures

Computer analysis

Putative Oca sequences were retrieved using PSI_Blast at the National Center for Biotechnology Information (NCBI) web site (http://www.ncbi.nlm.nih.gov/BLAST/) from the non-redundant protein database. Gene and protein sequence analysis was performed with the GCG Wisconsin Package suite (version 10.3). Secondary structure prediction on HadA was performed with the PHD algorithm available at the PredictProtein server (http://www.predictprotein.org/), and coiled-coil propensity was evaluated with Multicoil software (http://groups.csail.mit.edu/cb/multicoil/).

Bacterial strains and growth conditions

A collection of 58 strains identified according to phylogenetic analysis were used in the study: 15 *H. influenzae* biogroup *aegyptius* cluster strains, 6 of which were from fulminant invasive BPF infections (F3031, HK1183, HK1215, HK1216, HK1221, HK1222) and 9 from BPF-associated conjunctivitis (HK865, HK866, HK1219, HK1224, HK1227, HK1228, HK1232, HK1238, HK1239) all in Brazil; 2 isolates from Australian BPF-like infections HK1212 (199/88), HK1213 (F6422/349); 21 *H. aegyptius* strains isolated from cases of uncomplicated conjunctivitis in Texas, USA and Brazil (NCTC8502T, NCTC8134, HK1231, HK1248, HK1244, HK1247, HK1229, HK1249, HK1245, HK1246, NCTC8135, HK1234, HK1237, HK1233, HK1214, HK1241, F1947, HK1235, HK1236, HK1226, HK1240); 15 non-encapsulated/non-typeable *H. influenzae* strains, 10 of which were from cases of conjunctivitis in Tunesia and Denmark and the remaining from the upper respiratory tract (HK1220, HK292, HK284, HK295, HK272, HK286, ATCC19418, HK274, HK275, ATCC9134, HK266, NCTC8143^T, HK287, HK288, HK61); and 5 encapsulated *H. influenzae* strains of serotype b (NCTC8467, Division I) and HK368 (Division I), HK715 (Division II), serotype c (HK635), and originally serotype d, now rough strain Rd. *Haemophilus* strains were cultivated on chocolate agar polivitex (BioMerieux) incubated at 37°C with 5% CO_2. Brain–heart infusion (BHI) broth (Difco Laboratories) supplemented with 10 μg ml^{-1}, each of haemin (Fluka Biochemika) and nicotinamide adenine dinucleotide (NAD, Sigma), was used as fluid growth medium. *E. coli* strains DH5α, BL21(DE3) (Invitrogen) and HB101(DE3) were cultured at 37°C in Luria–Bertani (LB) medium and, when required, supplemented with 100 μg ml^{-1} ampicillin.

PCR and sequencing of hadA *region*

PCR amplification of the *hadA* locus was performed on bacterial colonies inactivated by boiling for 10 min. The Expand Long Template PCR System (Roche) was used. Amplification primes were homF and homR, mapping upstream and downstream *hadA* locus respectively. PCR conditions were: 5 cycles of denaturation at 94°C for 30 s, annealing at 54°C for 30 s, extension at 68°C for 3 min; 25 cycles of denaturation at 94°C for 30 s, annealing at 54°C for 30 s, extension at 68°C for 1 min. Time of elongation was increased, for the last 25 cycles, by 15 s per cycle. PCR products were analysed on agarose gel, purified using the Qiaquick PCR purification kit (QIAGEN) and sequenced by automated cyclo-sequenced (model 377; Applied Biosystems). Oligonucleotides used for sequencing were forward, HadA1, HadA2, HadA3, HadA4, and reverse primers, HadA5 and HadA6. Sequence analysis was performed using Vector NTI Explorer and ClustalX. Co-ordinates of changes were calculated by giving position 1 to the first nucleotide after primer homF.

Cell cultures

Tissue culture cells used in this study are Chang epithelial cells (Wong-Kilbourne derivative, clone 1–5c-4, human conjunctiva, ATCC CCL-20.2) and HUVECs. Chang cells were maintained in Dulbecco's modified Eagle's medium (DMEM; Gibco), supplemented with 25 mM Hepes, 15 mM L-glutamine, antibiotics and 10% (v/v) heat-inactivated fetal calf serum (FCS, Invitrogen Corporation). HUVECs were maintained in endothelial cell growth medium (M199+Earle's+L-glutamine, Gibco), supplemented with 20% (v/v) FCS, antibiotics, 2 ml l^{-1} heparin (Pfizer) and 100 mg l^{-1} bovine brain lyophilized extract. HUVECs were used between passage 1 and 5. All cells were grown at 37°C with 5% CO_2.

Plasmids construction and DNA manipulation

For the expression of all the recombinant proteins considered in this study, the specific DNA fragments were amplified by PCR using as template the chromosomal DNA from BPF strain F3031 and cloned into pET-21b+ expression vector (Novagen). DNA cloning and *E. coli* transformation was performed according to standard protocols. Restriction endonucleases and DNA-modifying enzymes were obtained from New England Biolabs and used according to the manufacturer's instructions. In order to express in *E. coli* the full-length HadA, the *hadA* gene was amplified using as primers the oligonucleotides *HadA*-Fwd and *HadA*-Rev: the PCR product obtained was digested with NdeI and XhoI restriction enzymes and inserted into the NdeI/XhoI sites of the pET-21b+ vector; the resulting construct was named pET-HadA.

HadA-His contains the *hadA* gene with sequence encoding the predicted leader peptide (amino acids 1–26) and the membrane anchor region (residues 204–256) deleted. The gene fragment (corresponding to amino acids 27–203), obtained by PCR using the *HadAhis*-Fwd and *HadAhis*-Rev primers, was digested with NdeI and XhoI and inserted into the pET-21b+ vector, as above. The plasmid was transformed in *E. coli* to express the protein as a C-terminal 6× His fusion.

The plasmids, containing the mutated genes coding for HadAΔ49-69, HadAΔ33-48, HadAΔ33-69, HadAΔ72-98 and HadAΔ99-132, were generated by a two-step cloning. PCRa (*HadA*-Fwd and *HadA48*-Rev, additional HindIII site; amplifying the region corresponding to amino acids 1–48) and PCRb (*HadA72*-Fwd additional HindIII site and *HadA*-Rev; amino acids 72–256) were used to express HadAΔ49-69. PCRc (*HadA*-Fwd and *HadA32*-Rev, additional NcoI site; amplifying the region corresponding to amino acids 1–32) and PCRd (*HadA49*-Fwd additional NcoI site and *HadA*-Rev; amino acids 49–256) were used to express HadAΔ33-48. PCRe (*HadA*-Fwd and *HadA32*-Rev, additional HindIII site; amplifying the region corresponding to amino acids 1–32) and PCRb were used to express HadAΔ33-69. PCRf (*HadA*-Fwd and *HadA69*-Rev, additional HindIII site; amplifying the region corresponding to amino acids 1–69) and PCRg (*HadA99*-Fwd additional HindIII site and *HadA*-Rev; amino acids 99–256) were used to express HadAΔ72-98. Finally, PCRh (*HadA*-Fwd and *HadA98*-Rev, additional EcoRV site; amplifying the region corresponding to amino acids 1–98) and PCRi (*HadA135*-Fwd additional EcoRV site and *HadA*-Rev; amino acids 135–256) were used to express HadAΔ99-132. No amino acids were inserted in the sequences as a result of the addition of the HindIII, NcoI and EcoRV sites. The amplified DNA fragments were digested with the appropriate restriction enzymes and cloned into the pET-21b+ vector digested with NdeI and XhoI enzymes.

The HadAΔKGD mutant, containing the *hadA* gene with the sequence corresponding to KGD motif deleted, was obtained by site-directed mutagenesis using the QuikChange Kit (Stratagene) and the pET-HadA construct as template. The HadA-AAA

mutant, corresponding to the point mutations for each single residue of the KGD motif, was obtained in the same way. The primers used for each of these constructs were *HadAΔKGD 1* and *HadAΔKGD 2*, *HadA-AAA 1* and *HadA-AAA 2* respectively. All the primers used in the PCR reactions described above are listed in Table S2.

Southern blot analysis

Southern hybridization analysis was performed as previously described (Kilian *et al*., 2002). The entire *hadA* gene, obtained by PCR amplification using F3031 genomic DNA as template, was used as a probe.

Gene expression, cell fractionation and protein analysis

For expression of HadA in BL21(DE3) strain, a single positive colony was inoculated in LB medium (supplemented with ampicillin) and grown overnight at 37°C; then bacteria were recovered by centrifugation. Protein expression was achieved without addition of IPTG, exploiting expression due to leakage of the induction system.

Haemophilus strains were grown in BHI overnight at 37°C with 5% CO_2 and recovered by centrifugation. Whole cell lysates were obtained by re-suspending 1 ml of bacteria in bacterial lysis buffer (20 mM Tris, 1 mM EDTA and 2% SDS; pH = 8.0) and boiling for 5–10 min.

Outer membrane proteins were recovered on the basis of Sarkosyl insolubility following the rapid procedure as described by Carlone *et al*. (1986). OMVs for Cryo-electron microscopy analysis were prepared as previously described (Davies *et al*., 1990).

Proteins were separated by SDS-PAGE electrophoresis using NuPAGE Gel System, according to the manufacturer's instructions (Invitrogen), and revealed by Coomassie blue staining or transferred onto nitrocellulose membranes for Western blot analysis.

Western blots were performed according to standard procedures. The different forms of HadA were identified with a polyclonal rabbit serum raised against recombinant HadA-His (diluted 1:1000) and an anti-rabbit serum conjugated to horseradish peroxidase (DAKO), as secondary antibody. Bands were visualized with Super Signal Chemiluminescent Substrate (Pierce) and with Opti 4 CN Substrate Kit (Bio-Rad) following the manufacturer's instructions.

Purification of recombinant HadA His fusion protein

For protein purification, one single colony of *E. coli* BL21(DE3) strain expressing HadA-His was inoculated in LB + ampicillin and grown overnight at 37°C, diluted in fresh LB medium and grown at 30°C to an OD of 0.6–0.8. The protein overexpression was induced by the addition of 1 mM isopropyl-1-thio-β-D-galactopyranoside (IPTG; Sigma) for 3 h. Recombinant HadA 6× His fusion protein was purified by affinity chromatography on Ni^{2+}-conjugated chelating fast-flow Sepharose 4B resin (Pharmacia). The purity was checked by SDS-PAGE electrophoresis staining with Coomassie blue. The protein content was quantified by Bradford reagent (Bio-Rad).

Preparation of polyclonal anti-HadA-His serum

To prepare rabbit anti-HadA-His serum, 25 μg of purified protein was used to immunize a New Zealand White rabbit. The recombinant protein was given subcutaneously with Freund's incomplete adjuvant for the first dose and with Freund's complete adjuvant for the second (day 21) and the third (day 35) booster doses. Blood sample was taken on day 49.

The treatments were performed in accordance with internal animal ethical committee and institutional guidelines. Finally, the serum was purified by affinity chromatography on CNBr activated Sepharose 4B resin (Pharmacia) according to the manufacturer's instructions.

Aggregation assay

A single colony of *E. coli* BL21(DE3) strain expressing HadA was inoculated in LB medium (supplemented with ampicillin) and grown overnight at 37°C, diluted in aliquots at OD_{600} = 1 and then left standing at room temperature for 5 h. To quantify the bacterial aggregation during this time, OD readings were performed at regular time intervals. Samples containing bacterial aggregates were spotted onto a well in six-well tissue culture plates (NUNC) and visualized by phase-contrast microscopy.

FACS analysis of bacteria

Surface detection of HadA in BPF F3031 and *E. coli* recombinant clones was performed using FACS analysis as previously described (Capecchi *et al*., 2005). Rabbit polyclonal anti-HadA-His serum, used as primary antibody and diluted 1:1000, was added directly to the cell suspension and incubated for 1 h at 4°C. After incubation with R-Phycoerythrin-conjugated anti-rabbit IgG, bacteria samples were washed twice, re-suspended in PBS and analysed with a FACSCalibur flow cytometer (Becton-Dickinson).

Infection of epithelial and endothelial cells: adhesion and invasion assays with E. coli *strains*

Chang conjunctiva epithelial cell (or HUVEC) suspensions obtained from confluent monolayers were seeded at 1.5×10^5 cells per well in 12-well tissue culture plates (NUNC) and incubated for 24 h in an antibiotics-free medium.

Overnight culture of bacteria were washed once and re-suspended in DMEM + 1% FCSi to a concentration of 3×10^7 bacteria ml^{-1} at a multiplicity of infection (moi) of approximately 1:100: aliquots of 1 ml of each strain were added to monolayer cultures of Chang cells (or HUVECs) and incubated for 3 h at 37°C in 5% CO_2.

Non-adherent bacteria were removed by washing three times with DMEM + 1% FCSi and twice with PBS. The remaining bacteria were released by addition of 1% Saponin (Sigma) and incubation at 37°C for 15 min: serial dilutions of the associated bacteria suspension were plated onto LB agar. Adhesion capability was quantified by counting colony-forming units (cfu).

To determine the number of intracellular bacteria in infected Chang (or HUVEC) monolayers, a Gentamicin survival invasion assay was performed as described previously (Capecchi *et al*., 2005).

Invasion assays in the presence of eukaryotic cytoskeleton inhibitors and clathrin KD cells

To investigate the role of eukaryotic cytoskeletal components in bacteria internalization, adhesion and invasion assays were performed in the presence of the actin microfilament inhibitor Cytochalasin D, the microtubule inhibitor Nocodazole and the tyrosine protein kinase inhibitor Genistein, as described elsewhere (Rosenshine *et al*., 1994).

Stock solutions of inhibitors were prepared at the following concentrations in Dimethyl Sulfoxide (Sigma) and stored in aliquots at –20°C until use: 1 mg ml^{-1} Cytochalasin D (Sigma), 1 mg ml^{-1} Nocodazole (Sigma), and 100 mM Genistein (Sigma). Prior to use the inhibitors were diluted in DMEM + 10% FCSi and added to cells. All inhibitors were pre-incubated with the cells for 30 min at 37°C prior to infection, and they were present throughout the infection period.

RNAi assay was performed as previously reported (Veiga *et al*., 2007). Briefly, double-stranded RNA against clathrin heavy-chain sense 5′-GGC CCA GGU GGU AAU CAU Utt-3′ and antisense 5′-AAU GAU UAC CAC CUG GGC Ctg-3′, and On-Target SMART pool against clathrin heavy chain (Dharmacon), or control RNA (Silencer Negative Control 1 siRNA; Ambion) and siCONTROL (Non-Targetting siRNA Pool; Dharmacon), were transfected into Chang cells using oligofectamin (Invitrogen) as recommended by the manufacturers. Chang cells were infected with *E. coli*-HadA 72 h after transfection. Colony-forming units were counting by plating cell lysates after gentamicin treatment.

Inhibition of adherence with anti-HadA antibodies

Cultures of *E. coli*-HadA were washed once with PBS, re-suspended in PBS and incubated with three different concentrations (1:1000, 1:100 and 1:10) of the rabbit polyclonal serum against HadA-His for 1 h at room temperature. As a negative control, bacteria were incubated with the same dilutions of a preimmune rabbit serum. Samples were washed with PBS, re-suspended in DMEM + FCSi, and used to infect Chang cells monolayers. The adhesion assay was performed as above. Inhibition of F3031 adhesion was performed as described for *E. coli* with the exceptions that the concentrations of anti-HadA antibodies were 1:5 and 1:2.

Inhibition of adherence by synthetic polypeptide

The nonameric peptide (-EKAKGDSSE-) comprising residues 93–101 of HadA was synthesized with a purity of > 95% (Primm). A peptide not containing a KGD sequence and designed on the aminoacidic sequence of the meningococcal NadA adhesin (23 aa) was used as negative control.

Monolayers of Chang cells were pre-incubated with EKAKGDSSE (0.01–0.3 mg ml^{-1}) or the control peptide (0.3 mg ml^{-1}) for 30 min at 37°C in DMEM + 1%FCS. Cells were examined following pre-incubation with the polypeptides to ensure no cell death or morphological changes. Subsequently, adhesion experiments were carried out as described above. The polypeptides were present throughout the infection experiment.

Cryo-electron microscopy analysis and image processing

Five microlitres of OMV preparation were loaded onto a glow discharged Quantifoil holey carbon grid with 2 μm holes and let stand for 5 min. After being blotted from the front side with a slip filter paper (Whatman No. 4), the grid was flash frozen into liquid ethane as described (Dubochet *et al*., 1988). The grids were observed using a CM200 FEG Philips Electron Microscope (FEI, Eindhoven, the Netherlands), equipped with a GATAN GIF 2002 post-column energy filter (Gatan, Pleasanton, CA, USA), and images were collected at an accelerating voltage of 200 kV and a nominal magnification of 50 000×, on Kodak SO163 film. Micrographs taken at 50 000× of magnification were digitized on an IMACON 949 scanner at spacing of 7.95 μm, resulting in a nominal sampling of 1.6 Å pixel/$^{-1}$. Single NadA and HadA were picked from digitized images using the command 'boxer' from the software EMAN (Ludtke *et al*., 1999) by using boxes of 64 × 64 pixels. The isolated NadA and HadA molecules were treated as single particles. In a first analysis, the boxed NadA and HadA molecules were aligned for classification and than subjected to high-pass and low-pass filtrations IMAGIC 5 (van Heel *et al*., 1996) and of Bsoft software. All the aligned and filtered images were consistent: the NadA images presented an elongated stalk decorated by a globular head, the HadA images presented instead a clove-like shape.

Scanning electron microscopy and transmission electron microscopy

For electron microscopy studies Chang epithelial cells were cultured on transwell filters (FALCON) and used at conditions identical to those used for adhesion experiments. After infection, polyethylene terephthalate membranes supporting the cells were cut by a scalpel and transferred into 1.5 ml Eppendorf tubes containing 2.5% glutaraldehyde and 2.5% paraformaldehyde in cacodylate sucrose buffer. Samples were fixed overnight and then kept at 4°C until being postfixed in 1% OsO_4 and 0.15% ruthenium red in cacodylate buffer. The samples were then blocked with 1% uranyl acetate and dehydrated with serial concentrations of acetone.

For SEM, samples were then dried by the critical point method using CO_2 in a Balzers Union CPD 020, sputter-coated with gold in a Balzers MED 010 unit, and observed with a JEOL JSM 5200 electron microscope. For TEM, samples were fixed and dehydrated as described above then embedded in Epon-based resin. Thin sections were cut with a Reichert Ultracut ultramicrotome by use of a diamond knife, collected on collodion copper grids, stained with uranyl acetate and lead citrate, and observed with a JEOL 1200 EX II electron microscope.

Immunoelectron microscopy

For immunoelectron microscopy, samples were fixed with a mixture of 1% glutaraldehyde and 4% paraformaldehyde in 0.1 M phosphate buffer pH 7.2 for 2 h at room temperature. After rinsing in the same buffer for 10 min, samples were dehydrated in a graded ethanol series and embedded in medium-grade LR White resin (Multilab Supplies, Surrey, England). The resin was polymerized in tightly capped gelatin capsules for 48 h at 50°C.

Thin sections were obtained using a Reichert Ultracut ultramicrotome with a diamond knife, and collected on nickel grids.

For Immunogold staining, non-specific antigens were blocked with Tris buffer (0.05 M, pH 7.6) containing 0.5% BSA for 15 min. Sections were incubated overnight in a moist chamber with rabbit polyclonal anti-HadA-His serum diluted 1:1000 in Tris buffer containing 0.2% BSA. The primary antibody was omitted in negative control sections. The grids were washed in Tris buffer for 20 min, then in Tris buffer containing 0.1% BSA for 10 min. Sections were incubated with a secondary goat anti-rabbit antibody conjugated to 10 nm gold particles (British Biocell International, UK), diluted 1:100 in 0.02 M, pH 8.2 Tris buffer. After rinsing in 0.05 M Tris buffer containing 0.1% BSA for 10 min and in 0.05 M Tris buffer for 20 min, the grids were washed three times with distilled water (for 5 min). Sections were stained with uranyl acetate and observed with a Jeol JEM EX II transmission electron microscope.

Binding to ECM proteins: quantitative adherence assay

In assays examining adherence to ECM proteins we considered five proteins: Collagens I, III and VI (Sigma) as collageneous proteins, fibronectin (from human plasma, Sigma) and laminin (from basement membrane, Sigma) as non-collageneous proteins. The adherence to ECM proteins was quantified by plating and counting bacteria: 1 day before the experiment 96-well tissue culture plates (flat bottom, Costar) were coated at 4°C with 0.1 mg ml^{-1} of each type of selected ECM proteins. Bacterial suspensions grown to late exponential phase were washed and re-suspended in PBS + 1% FCSi, added to plates and incubated for 3 h at 37°C. After incubation, they were washed three times with PBS to remove non-adherent bacteria, and then harvested with trypsin-EDTA (0.05% trypsin – 0.5% EDTA, Gibco) to release adherent bacteria from the support; serial dilutions of them were plated onto LB agar.

Nucleotide sequence accession numbers

The sequences corresponding to *hadA* region of F3031, F1947, Eagan and NT36 strains have been deposited in the GenBank and the assigned accession numbers are EU998937, EU998938, EU998939 and EU998940 respectively.

Acknowledgements

We thank Simon J. Kroll for providing chromosomal DNA from some *Haemophilus* strains, Kate L. Seib for helpful discussion and critical reading of the manuscript, Claudia Trappetti and Francesca Morandi for technical help and Giorgio Corsi for artwork.

References

Abu el-Asrar, A.M., Geboes, K., al-Kharashi, S.A., al-Mosallam, A.A., Tabbara, K.F., al-Rajhi, A.A., and Missotten, L. (1998) An immunohistochemical study of collagens in trachoma and vernal keratoconjunctivitis. *Eye* **12:** 1001–1006.

Abu El-Asrar, A.M., Meersschaert, A., Al-Kharashi, S.A., Missotten, L., and Geboes, K. (2003) Immuno-histochemical evaluation of conjunctival remodelling in vernal keratoconjunctivitis. *Eye* **17:** 767–771.

Bliska, J.B., Copass, M.C., and Falkow, S. (1993a) The *Yersinia pseudotuberculosis* adhesin YadA mediates intimate bacterial attachment to and entry into HEp-2 cells. *Infect Immun* **61:** 3914–3921.

Bliska, J.B., Galan, J.E., and Falkow, S. (1993b) Signal transduction in the mammalian cell during bacterial attachment and entry. *Cell* **73:** 903–920.

Brenner, D.J., Mayer, L.W., Carlone, G.M., Harrison, L.H., Bibb, W.F., Brandileone, M.C., *et al.* (1988) Biochemical, genetic, and epidemiologic characterization of *Haemophilus influenzae* biogroup *aegyptius* (*Haemophilus aegyptius*) strains associated with Brazilian purpuric fever. *J Clin Microbiol* **26:** 1524–1534.

Capecchi, B., Adu-Bobie, J., Di Marcello, F., Ciucchi, L., Masignani, V., Taddei, A., *et al.* (2005) *Neisseria meningitidis* NadA is a new invasin which promotes bacterial adhesion to and penetration into human epithelial cells. *Mol Microbiol* **55:** 687–698.

Carlone, G.M., Thomas, M.L., Rumschlag, H.S., and Sottnek, F.O. (1986) Rapid microprocedure for isolating detergent-insoluble outer membrane proteins from Haemophilus species. *J Clin Microbiol* **24:** 330–332.

CDC (1985) Preliminary report: epidemic fatal purpuric fever among children – Brazil. *MMWR Morb Mortal Wkly Rep* **34:** 217–219.

Comanducci, M., Bambini, S., Brunelli, B., Adu-Bobie, J., Arico, B., Capecchi, B., *et al.* (2002) NadA, a novel vaccine candidate of *Neisseria meningitidis*. *J Exp Med* **195:** 1445–1454.

Cornelis, G.R., Boland, A., Boyd, A.P., Geuijen, C., Iriarte, M., Neyt, C., *et al.* (1998) The virulence plasmid of *Yersinia*, an antihost genome. *Microbiol Mol Biol Rev* **62:** 1315–1352.

Cossart, P., and Sansonetti, P.J. (2004) Bacterial invasion: the paradigms of enteroinvasive pathogens. *Science* **304:** 242–248.

Cotter, S.E., Surana, N.K., and St Geme, J.W., 3rd (2005) Trimeric autotransporters: a distinct subfamily of autotransporter proteins. *Trends Microbiol* **13:** 199–205.

Davies, R.L., Wall, R.A., and Borriello, S.P. (1990) Comparison of methods for the analysis of outer membrane antigens of *Neisseria meningitidis* by western blotting. *J Immunol Meth* **134:** 215–225.

Desvaux, M., Parham, N.J., and Henderson, I.R. (2004) The autotransporter secretion system. *Res Microbiol* **155:** 53–60.

Dubochet, J., Adrian, M., Chang, J.J., Homo, J.C., Lepault, J., McDowall, A.W., and Schultz, P. (1988) Cryo-electron microscopy of vitrified specimens. *Q Rev Biophys* **21:** 129–228.

Eitel, J., and Dersch, P. (2002) The YadA protein of *Yersinia pseudotuberculosis* mediates high-efficiency uptake into human cells under environmental conditions in which invasin is repressed. *Infect Immun* **70:** 4880–4891.

El Tahir, Y.S.M. (2001) YadA, the multifaceted *Yersinia* adhesin. *Int J Med Microbiol* **291:** 209–218.

Farley, M.M., Whitney, A.M., Spellman, P., Quinn, F.D., Weyant, R.S., Mayer, L., and Stephens, D.S. (1992) Analy-

sis of the attachment and invasion of human epithelial cells by *Haemophilus influenzae* biogroup *aegyptius*. *J Infect Dis* **165** (Suppl. 1)**:** S111–S114.

Frankel, G., Lider, O., Hershkoviz, R., Mould, A.P., Kachalsky, S.G., Candy, D.C., *et al.* (1996) The cell-binding domain of intimin from enteropathogenic *Escherichia coli* binds to beta1 integrins. *J Biol Chem* **271:** 20359–20364.

Girard, V., and Mourez, M. (2006) Adhesion mediated by autotransporters of Gram-negative bacteria: structural and functional features. *Res Microbiol* **157:** 407–416.

Group, T.B.P.F.S. (1992) Brazilian purpuric fever identified in a new region of Brazil. The Brazilian Purpuric Fever Study Group. *J Infect Dis* **165** (Suppl. 1)**:** S16–S19.

Harrison, L.H., Simonsen, V., and Waldman, E.A. (2008) Emergence and disappearance of a virulent clone of *Haemophilus influenzae* biogroup *aegyptius*, cause of Brazilian purpuric fever. *Clin Microbiol Rev* **21:** 594–605.

Hasman, H., Chakraborty, T., and Klemm, P. (1999) Antigen-43-mediated autoaggregation of *Escherichia coli* is blocked by fimbriation. *J Bacteriol* **181:** 4834–4841.

van Heel, M., Harauz, G., Orlova, E.V., Schmidt, R., and Schatz, M. (1996) A new generation of the IMAGIC image processing system. *J Struct Biol* **116:** 17–24.

Heise, T., and Dersch, P. (2006) Identification of a domain in *Yersinia* virulence factor YadA that is crucial for extracellular matrix-specific cell adhesion and uptake. *Proc Natl Acad Sci USA* **103:** 3375–3380.

Hill, D.J., and Virji, M. (2003) A novel cell-binding mechanism of *Moraxella catarrhalis* ubiquitous surface protein UspA: specific targeting of the N-domain of carcinoembryonic antigen-related cell adhesion molecules by UspA1. *Mol Microbiol* **48:** 117–129.

Hill, D.J., Edwards, A.M., Rowe, H.A., Virji M. (2005) Carcinoembryonic antigen-related cell adhesion molecule (CEACAM)-binding recombinant polypeptide confers protection against infection by respiratory and urogenital pathogens. *Mol Microbiol* **55:** 1515–1527.

Hoiczyk, E., Roggenkamp, A., Reichenbecher, M., Lupas A., and Heesemann, J. (2000) Structure and sequence analysis of *Yersinia* YadA and *Moraxella* UspAs reveal a novel class of adhesins. *EMBO J* **19:** 5989–5999.

Iriarte, M., and Cornelis, G.R. (1996) Molecular determinants of *Yersinia* pathogenesis. *Microbiologia* **12:** 267–280.

Kilian, M., Poulsen, K., and Lomholt, H. (2002) Evolution of the paralogous *hap* and *iga* genes in *Haemophilus influenzae*: evidence for a conserved *hap* pseudogene associated with microcolony formation in the recently diverged *Haemophilus aegyptius* and *H. influenzae* biogroup *aegyptius*. *Mol Microbiol* **46:** 1367–1380.

Klemm, P., Vejborg, R.M., and Sherlock, O. (2006) Self-associating autotransporters, SAATs: functional and structural similarities. *Int J Med Microbiol* **296:** 187–195.

Laarmann, S., Cutter, D., Juehne, T., Barenkamp S.J., and St Geme, J.W., III (2002) The *Haemophilus influenzae* Hia autotransporter harbours two adhesive pockets that reside in the passenger domain and recognize the same host cell receptor. *Mol Microbiol* **46:** 731–743.

Lafontaine, E.R., Cope, L.D., Aebi, C., Latimer, J.L., and McCracken, G.H., Jr, and Hansen, E.J. (2000) The UspA1 protein and a second type of UspA2 protein mediate adherence of *Moraxella catarrhalis* to human epithelial cells *in vitro*. *J Bacteriol* **182:** 1364–1373.

Li, L., Matevski, D., Aspiras, M., Ellen, R.P., and Lepine, G. (2004) Two epithelial cell invasion-related loci of the oral pathogen *Actinobacillus* actinomycetemcomitans. *Oral Microbiol Immunol* **19:** 16–25.

Li, M.S., Farrant, J.L., Langford, P.R., and Kroll, J.S. (2003) Identification and characterization of genomic loci unique to the Brazilian purpuric fever clonal group of *H. influenzae* biogroup *aegyptius*: functionality explored using meningococcal homology. *Mol Microbiol* **47:** 1101–1111.

Linke, D., Riess, T., Autenrieth, I.B., Lupas, A., and Kempf, V.A. (2006) Trimeric autotransporter adhesins: variable structure, common function. *Trends Microbiol* **14:** 264–270.

Ludtke, S.J., Baldwin, P.R., and Chiu, W. (1999) EMAN: semiautomated software for high-resolution single-particle reconstructions. *J Struct Biol* **128:** 82–97.

McMichael, J.C., Fiske, M.J., Fredenburg, R.A., Chakravarti, D.N., VanDerMeid, K.R., Barniak, V., *et al.* (1998) Isolation and characterization of two proteins from *Moraxella catarrhalis* that bear a common epitope. *Infect Immun* **66:** 4374–4381.

Nykvist, P., Tasanen, K., Viitasalo, T., Kapyla, J., Jokinen, J., Bruckner-Tuderman, L., and Heino, J. (2001) The cell adhesion domain of type XVII collagen promotes integrin-mediated cell spreading by a novel mechanism. *J Biol Chem* **276:** 38673–38679.

Ochiai, K., Kurita-Ochiai, T., Kamino, Y., and Ikeda, T. (1993) Effect of co-aggregation on the pathogenicity of oral bacteria. *J Med Microbiol* **39:** 183–190.

Quinn, F.D., Weyant, R.S., Worley, M.J., White, E.H., Utt, E.A., and Ades, E.A. (1995) Human microvascular endothelial tissue culture cell model for studying pathogenesis of Brazilian purpuric fever. *Infect Immun* **63:** 2317–2322.

Ray, S.K., Rajeshwari, R., Sharma, Y., and Sonti, R.V. (2002) A high-molecular-weight outer membrane protein of *Xanthomonas oryzae* pv. *oryzae* exhibits similarity to non-fimbrial adhesins of animal pathogenic bacteria and is required for optimum virulence. *Mol Microbiology* **46:** 637–647.

Relman, D., Tuomanen, E., Falkow, S., Golenbock, D.T., Saukkonen, K., and Wright, S.D. (1990) Recognition of a bacterial adhesion by an integrin: macrophage CR3 (alpha M beta 2, CD11b/CD18) binds filamentous hemagglutinin of *Bordetella pertussis*. *Cell* **61:** 1375–1382.

Riess, T., Andersson, S.G., Lupas, A., Schaller, M., Schafer, A., Kyme, P., *et al.* (2004) *Bartonella* adhesin a mediates a proangiogenic host cell response. *J Exp Med* **200:** 1267–1278.

Roggenkamp, A., Ackermann, N., Jacobi, C.A., Truelzsch, K., Hoffmann, H., and Heesemann, J. (2003) Molecular analysis of transport and oligomerization of the *Yersinia enterocolitica* adhesin YadA. *J Bacteriol* **185:** 3735–3744.

Rosenshine, I., Donnenberg, M.S., Kaper, J.B., and Finlay, B.B. (1992a) Signal transduction between enteropathogenic *Escherichia coli* (EPEC) and epithelial cells: EPEC induces tyrosine phosphorylation of host cell proteins to initiate cytoskeletal rearrangement and bacterial uptake. *Embo J* **11:** 3551–3560.

Rosenshine, I., Duronio, V., and Finlay, B.B. (1992b) Tyrosine protein kinase inhibitors block invasin-promoted

bacterial uptake by epithelial cells. *Infect Immun* **60:** 2211–2217.

Rosenshine, I., Ruschkowski, S., and Finlay, B.B. (1994) Inhibitors of cytoskeletal function and signal transduction to study bacterial invasion. *Meth Enzymol* **236:** 467–476.

Scarselli, M., Serruto, D., Montanari, P., Capecchi, B., Adu-Bobie, J., Veggi, D., *et al.* (2006) *Neisseria meningitidis* NhhA is a multifunctional trimeric autotransporter adhesin. *Mol Microbiol* **61:** 631–644.

Segada, L.M., and Lesse, A.J. (1997) Creation of an isogenic P1-deficient mutant of *Haemophilus influenzae* biogroup *aegyptius*. *Gene* **204:** 185–194.

Sherlock, O., Schembri, M.A., Reisner, A., and Klemm, P. (2004) Novel roles for the AIDA adhesin from diarrheagenic *Escherichia coli*: cell aggregation and biofilm formation. *J Bacteriol* **186:** 8058–8065.

Sherlock, O., Vejborg, R.M., and Klemm, P. (2005) The TibA adhesin/invasin from enterotoxigenic *Escherichia coli* is self recognizing and induces bacterial aggregation and biofilm formation. *Infect Immun* **73:** 1954–1963.

Skurnik, M., el Tahir, Y., Saarinen, M., Jalkanen, S., and Toivanen, P. (1994) YadA mediates specific binding of enteropathogenic *Yersinia enterocolitica* to human intestinal submucosa. *Infect Immun* **62:** 1252–1261.

Smoot, L.M., Franke, D.D., McGillivary, G., and Actis, L.A. (2002) Genomic analysis of the F3031 Brazilian purpuric fever clone of *Haemophilus influenzae* biogroup *aegyptius* by PCR-based subtractive hybridization. *Infect Immun* **70:** 2694–2699.

St Geme, J.W., 3rd, Gilsdorf J.R., and Falkow, S. (1991) Surface structures and adherence properties of diverse strains of *Haemophilus influenzae* biogroup *aegyptius*. *Infect Immun* **59:** 3366–3371.

Surana, N.K.Cutter, D., Barenkamp S.J., and St Geme, J.W., III (2004) The *Haemophilus influenzae* Hia autotransporter contains an unusually short trimeric translocator domain. *J Biol Chem* **279:** 14679–14685.

Szczesny, P., and Lupas, A. (2008) Domain annotation of trimeric autotransporter adhesins – daTAA. *Bioinformatics (Oxford, England)* **24:** 1251–1256.

Veiga, E., and Cossart, P. (2005) Listeria hijacks the clathrin-dependent endocytic machinery to invade mammalian cells. *Nature Cell Biology* **7:** 894–900.

Veiga, E., and Cossart, P. (2006) The role of clathrin-dependent endocytosis in bacterial internalization. *Trends Cell Biology* **16:** 499–504.

Veiga, E., Guttman, J.A., Bonazzi, M., Boucrot, E., Toledo-Arana, A., Lin, A.E., *et al.* (2007) Invasive and adherent bacterial pathogens co-Opt host clathrin for infection. *Cell Host Microbe* **2:** 340–351.

Weyant, R.S., Bibb, W.F., Stephens, D.S., Holloway, B.P., Moo-Penn, W.F., Birkness, K.A., *et al.* (1990) Purification and characterization of a pilin specific for Brazilian purpuric fever-associated *Haemophilus influenzae* biogroup *aegyptius* (*H. aegyptius*) strains. *J Clin Microbiol* **28:** 756–763.

Whitney, A.M., and Farley, M.M. (1993) Cloning and sequence analysis of the structural pilin gene of Brazilian purpuric fever-associated *Haemophilus influenzae* biogroup *aegyptius*. *Infect Immun* **61:** 1559–1562.

Yang, Y., and Isberg, R.R. (1993) Cellular internalization in the absence of invasin expression is promoted by the *Yersinia pseudotuberculosis* yadA product. *Infect Immun* **61:** 3907–3913.

Zhang, P., Chomel, B.B., Schau, M.K., Goo, J.S., Droz, S., Kelminson, K.L., *et al.* (2004) A family of variably expressed outer-membrane proteins (Vomp) mediates adhesion and autoaggregation in *Bartonella quintana*. *Proc Natl Acad Sci USA* **101:** 13630–13635.

Supporting information

Additional Supporting Information may be found in the online version of this article:

Fig. S1. HadA protein structure and comparison with close homologues. HadA protein structure in comparison with *N. meningitidis* NadA and *A. actinomycetemcomitans* ApiA proteins. The leader peptide is in white, the predicted head domain is grey, the coiled-coil stalk is hatched, and the membrane-anchor is black. Protein lengths are in scale. The coiled-coil prediction for each protein is reported above as a graph of probability scores, as obtained from the Paircoil server (http://groups.csail.mit.edu/cb/paircoil2/paircoil2.html). Numbers within the anchor domain indicate the % identity of this region with respect to the corresponding segment of HadA.

Fig. S2. Prediction and comparison of the α-helix coiled-coil of HadA and NadA passenger domains. The profile of different propensities to form dimeric and trimeric coiled-coil super-secondary structures has been calculated using Multicoil software (http://groups.csail.mit.edu/cb/multicoil/).

Table S1. Comprehensive list of TCcA proteins retrieved with Blast screening. *Several hits are detected within the *Haemophilus somnus* genomes. Hits corresponding to unannotated members of TCcA family are shown in bold.

Table S2. Oligonucleotides used in this study. Restriction sites are underlined in the sequence.

Please note: Wiley-Blackwell are not responsible for the content or functionality of any supporting materials supplied by the authors. Any queries (other than missing material) should be directed to the corresponding author for the article.